PHOTO-IONIZATION AND RYDBERG STATES OF TETRAAMINOETHYLENES IN THE GAS PHASE AND IN SOLUTIONS.

by

Yoshihiro NAKATO

Department of Chemistry

Faculty of Engineering Science

Osaka University

December, 1971

論　文　目　録

大阪大学

報告番号	乙第1082号	氏名	中　戸　義　禮

主論文　Photo-Ionization and Rydberg States of Tetra-aminoethylenes in the Gas Phase and in Solutions.
(気相および溶液中におけるテトラアミノエチレン類の光イオン化とリドベルグ状態)

欧文題名　Ionization Energies and Rydberg States of Tetraaminoethylenes. (テトラアミノエチレン類のイオン化エネルギーとリドベルグ状態)
原稿. 27枚
Bull. Chem. Soc. Japan, Vol. 45, No. 5.
昭和47年5月掲載の予定.

欧文題名　Photo-ionization and Rydberg States of Tetra-aminoethylenes in Organic Solutions. (有機溶液中でのテトラアミノエチレン類の光イオン化とリドベルグ状態)
原稿　27枚
J. Phys. Chem.,　投稿中.

参考論文

欧文題名　The Photo-ionization of N,N,N',N'-Tetramethyl-p-phenylenediamine in Organic Matrices.
(有機マトリックス中でのN,N,N',N'-テトラメチル-p-フェニレンジアミンの光イオン化).
坪村宏他6名と共著, Bull. Chem. Soc. Japan, Vol. 38, No. 11, p. 2021 (1965).

欧文題名　The Photo-ionization of Molecules in Solutions. II. Electron Transfer from Aromatic Diamine to Pyrene.

(溶液中での分子の光イオン化. II. 芳香族ジアミンからピレンへの電子移動)
坪村 宏 他1名と共著, Bull. Chem. Soc. Japan, Vol. 39, No. 5, p. 1092 (1966).

欧文題名 The Photo-ionization of Molecules in Solutions. III. Photo-ionization and Recombination Processes of N, N, N', N'-Tetramethyl-p-phenylenediamine in Various Organic Solvents. (溶液中での分子の光イオン化. III. 種々の有機溶媒中でのN,N,N',N'-テトラメチル-p-フェニレンジアミンの光イオン化と再結合過程.)
坪村 宏 他1名と共著, Bull. Chem. Soc. Japan, Vol. 39, No. 12, p. 2603-2608 (1966).

欧文題名 The Photo-ionization of Molecules in Solutions. IV. Electron Capture and Charge Transfer Fluorescence Phenomena Occurring between N, N, N', N'-Tetramethyl-p-phenylenediamine and Electron Acceptors in Organic Solvents. (溶液中での分子の光イオン化 IV. 有機溶媒中において N,N,N',N'-テトラメチル-p-フェニレンジアミンと電子受容体との間で生ずる電子捕獲および電荷移動ケイ光現象.
坪村 宏 他1名と共著, Bull. Chem. Soc. Japan, Vol. 40, No. 3, p. 451-455 (1967).

欧文題名 The Photo-ionization of Molecules in Solutions. V. The Mechanism of the Photo-ionization of an Aromatic Diamine in the Polar Solvents. (溶液中での分子の光イオン化. V. 極性溶媒中での芳香族ジアミンの光イオン化

のメカニズム）

坪村 宏 他1名と共著, Bull. Chem. Soc. Japan, Vol. 40, No. 11, p. 2480－2485 (1967).

欧文題名 Absorption Spectrum of Pyrene in the Excited Singlet State Measured by the Flash Method. （フラッシュ法で測定された 励起一重項状態のピレンの吸収スペクトル）

坪村 宏 他1名と共著, Chem. Phys. Letters, Vol. 2, No. 1, p. 57－58 (1968).

欧文題名 Solvent Effects on the Fluorescence Spectra of Some Aliphatic Amines in Solutions. （溶液中でのいくつかの脂肪族アミンのケイ光スペクトルに対する溶媒効果）

坪村 宏 他1名と共著, Chem. Phys. Letters, Vol. 9, No. 6, p. 597－599 (1971).

欧文題名 Organic Amino Compounds with Very Low Ionization Potentials. （非常に低い イオン化ポテンシャルをもった 有機アミノ化合物）

坪村 宏 他1名と共著, Chem. Phys. Letters, Vol. 9, No. 6, p. 615－616 (1971).

PHOTO-IONIZATION AND RYDBERG STATES OF TETRAAMINOETHYLENES IN THE GAS PHASE AND IN SOLUTIONS.

by

Yoshihiro NAKATO

Department of Chemistry

Faculty of Engineering Science

Osaka University

December, 1971

Contents

Preface

Studies on the photo-ionization of organic molecules in solutions,

$$M + h\nu \longrightarrow M^{+} + e,$$

have been of growing importance, directly connected with the electronic structures and processes of highly excited states of molecules and their aggregates. The knowledge on both the ionization mechanisms and the ionized states might also serve for the development of photo-sensitive organic materials or systems, on which much attention has recently been focused.

Extensive studies on the photo-ionization and related phenomena have been made in the last decade, stimulated by recent great developments of photochemistry, photophysics and radiation chemistry as well as by new experimental methods such as flash and laser techniques. Main results obtained so far may be summarized as follows; (1) Light in the near UV region can ionize some aromatic compounds by a two-step, biphotonic process with the triplet state as the intermediate. (2) Photo-ejected electrons are trapped in rigid organic matrices at fairly large distances (30 - 100 Å) from the parent cations. (3) Recombination processes of the trapped electrons with the parent cations, caused thermally as well as by illumination of IR light or by application of electric field, form the excited singlet

and triplet states of the parent molecules, emitting the fluorescence and phosphorescence. (4) The photo-ejected electrons have relatively high drift mobilities (0.1 - 100 $cm^2V^{-1}sec^{-1}$) in some non-polar organic solvents, which are the same as or even higher than those in organic crystals.

There are still difficulties in the studies on the photo-ionization in organic media, mainly because the photo-ionized and "Rydberg" states generally lie in the range of low-lying valence excited states of both solute and solvent molecules. For this reason, the determination of such basic quantities as the ionization thresholds and ionization yields in solutions has been left untouched. The studies on the "Rydberg" states connected with the ionization continua have also been undeveloped. Almost no studies have been made concerning the relations between these ionized and "Rydberg" states and CT complexes (or interactions), although the relations between the lower excited states and CT states have been well-established.

The present author has found that tetraaminoethylenes have extremely low gas-phase ionization potentials ($\sim$ 5.4 eV), to his knowledge, the lowest of the ionization potentials of organic molecules reported so far. These compounds have also very low Rydberg states lying near the visible region. These remarkable properties of these

molecules are not only very suitable for the detailed studies on the photo-ionization processes in organic media, but also offer an interesting example for searching materials with very low ionization potentials.

In the first chapter, the results of measurements of the photo-ionization curves, ionization potentials and absorption spectra of the tetraaminoethylenes in the gas phase are presented, together with the discussions on the electronic structures and ionization potentials based on the MO calculations of these molecules.

In the second chapter, the results of measurements of absorption and emission spectra and photo-ionization curves of tetraaminoethylenes in organic solvents are presented. The ionization continua, the "Rydberg" states, the contact CT states and their inter-relations in organic media are also discussed.

Chapter I

Ionization Energies and Rydberg States of Tetraaminoethylenes in the Gas Phase.

Summary

Absorption spectra and photo-ionization curves of tetrakis-(dimethylamino)-ethylene, (TMAE) and 1, 1', 3, 3'-tetramethyl-$\Delta^{2,2'}$-bi(imidazolidine), (TMBI) have been studied. It has been found that these compounds have very low ionization potentials (about 5.4 eV), which are even comparable with that of the lithium atom. The first ionization potentials of these compounds are nearly the same, although both their absorption spectra and their photo-ionization curves are considerably different from each other. These results can be explained semi-quantitatively by use of the results of simple, semi-empirical molecular orbital calculation with inclusion of direct interaction between four lone-pair orbitals on the N atoms, which was found to be important at the "perpendicular" structure. The first absorption bands of these molecules are assigned to the Rydberg bands,

lying quite unusually near the visible region. The quantum defect δ is found to be 0.7 for the lowest Rydberg state of TMAE. The size of the Rydberg orbital for this state is estimated to be 2.9 Å from the maximum radial density, which are comparable with the core size. Higher Rydberg series are also observed for TMBI.

Introduction

Ionization potentials of organic compounds are one of the key quantities in the studies of electronic processes in organic materials, such as organic semi-conductors, organic photo-conductors, and formation and reactions of electron-donor-acceptor complexes. The gas-phase ionization potentials of organic compounds reported so far lie in the range of about 7 to 12 eV.[1] The present author has found that tetrakis-(dimethylamino)-ethylene, (TMAE), and 1,1',3,3'-tetramethyl-$\Delta^{2,2'}$-bi(imidazolidine), (TMBI), have extremely low ionization potentials, about 5.4 eV, in spite of their relatively simple molecular structures.[2]

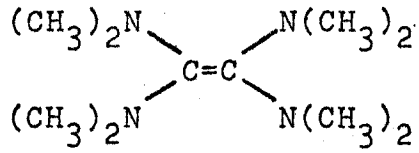

TMAE

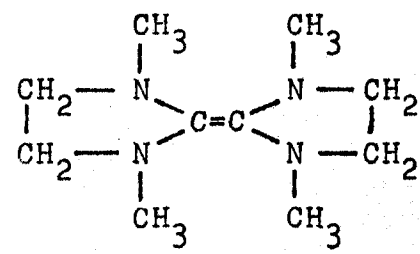

TMBI

The fact that dialkylamino groups have strong electron

donating properties is well known. Tetraaminoethylenes have as many such groups as possible for a substituted ethylene, and hence are very strong electron-donors. The chemical properties of these interesting compounds have been studied extensively and they are characterized as electron-rich olefins[3] or as strong electron donors.[4]

The knowledge on the electronic structures of tetraaminoethylenes is, however, still rather limited. The electron donor strength, the bonding and the electronic spectra for TMAE were interpreted by a simple HMO calculation.[4] The electronic spectra were also explained qualitatively in terms of intramolecular charge transfer mechanism.[5]

There have been some difficulties, both experimental and theoretical, in the study of the electronic structure of the tetraaminoethylenes. In the first place, they are strongly reactive to oxygen, emitting strong luminescences. The experiments with them must, therefore, be made with extreme carefulness. Secondly, there is some ambiguity as to their molecular conformations. It is expected that a large steric repulsion exists between four dialkylamino groups. This may prevent the tetraaminoethylenes from taking the "planar" structures and make their conformations more or less uncertain. The "non-planar" structure may lead to a breakdown of the π-electron approximation. Namely, the lone-pair orbitals on the N atoms overlap not only with

the π-orbitals on the C atoms, but also directly with the other lone-pair orbitals, and with the σ-orbitals. Finally, the role of the molecular Rydberg states in the low-lying excited levels has been overlooked.

In the present chapter, the results of measurements on the photo-ionization curves, ionization potentials and absorption spectra will be described, together with the discussions on the electronic structures and ionization potentials of free molecules in the gas phase, based on the MO calculations of these molecules.

Experimental

Both TMAE and TMBI were prepared according to the literature.[6] Crude products were distilled in an atmosphere of nitrogen under reduced pressure. They were then degassed and distilled repeatedly in a vacuum line, and stored in evacuated glass ampoules with breakable seals. n-Pentane, isopentane and methylcyclohexane were passed through silica-gel columns, left overnight in contact with sodium wire and distilled. All the sample solutions were prepared by dissolving TMAE or TMBI through breakable seals into solvents after they had been completely deoxygenated. Absorption spectra of TMAE and TMBI at room temperature were measured by using various cells with pass length ranging from 1.0 to 10 cm.

Absorption spectra in the wavelength region longer

than 190 nm were measured in a Cary Model 15 spectrophotometer. Both absorption spectra and photo-ionization curves in the wavelength region between 300 and 155 nm were measured by a 0.5 meter Nalumi vacuum monochromator. It has a Bausch and Lomb concave grating (concave radius 498.1 mm, ruled area 30 mm X 51 mm, 600 grooves/mm, blazed at 1500 Å, blaze angle 2°35'). The plate factor of the monochromator is calculated to be 28.3 Å/mm when the grating is used in the first order at λ = 150 nm. The slit width used was normally 200 μ. The light source used is a hot-cathode-type hydrogen-discharge lamp from Mitsubish Electric Corp., operated at 0.9 A and 70 V, which emits photons of the wavelengths longer than 155 nm. A Toshiba 7696 photomultiplier (S-11 type) covered with a sodium salicylate thin film is used as a photon detector. Emission lines from mercury and hydrogen lamps were used to calibrate the wavelength scale. The stray light was found to be less than 3 % of the total light from the exit slit around 160 and 180 nm.

Photon absorption and photocurrent were measured as functions of photon energy in the same run. A pyrex cell used has two quartz windows (transparent down to 155 nm) and two collecting-electrodes held parallel to each other by means of tungsten wire-pyrex seals, the resistance between which was 3 X 10^{15} ohms at 25 °C. Photocurrent was measured with a Takeda Riken vibrating reed electrometer, TR-84M. The

applied voltage between electrodes was 5 to 10 V in normal use. Under the above experimental conditions, the minimum photocurrent detected was about 2.0×10^{-15} A. Estimating the light intensity at some 10^9 photons/sec from the photomultiplier output, the photo-ionization yield ($=\sigma_i/\sigma$) can be measured to be at least 2×10^{-5}, if it is assumed roughly that one half the incident light was absorbed by the sample vapor (where σ and σ_i are absorption and photo-ionization cross sections, respectively).

Results

An absorption spectrum of TMAE in the vapor phase is shown in Fig. 1. At least four transitions may be involved in the spectrum which are centered at 29.0, 38.5, 44.8 and 53.0 kK. The first (29.0 kK) and the second (38.5 kK) bands agree closely with those reported by Winberg, Downing, Coffman,[7] and the fourth (53.0 kK) agrees with that by Hori, Kimura and Tsubomura.[5] Some structures are seen in the region around the fourth band. Near ultraviolet absorption spectra of TMAE in MP solutions, both at room temperature and 77°K, are given in Fig. 2 together with that in the gas phase, where MP is a mixed solvent consisting of methylcyclohexane and isopentane in a volume ratio of 1 : 1. A similar spectrum was obtained in an n-pentane solution or in an ether solution, and a maximum was found at 45.5 kK.

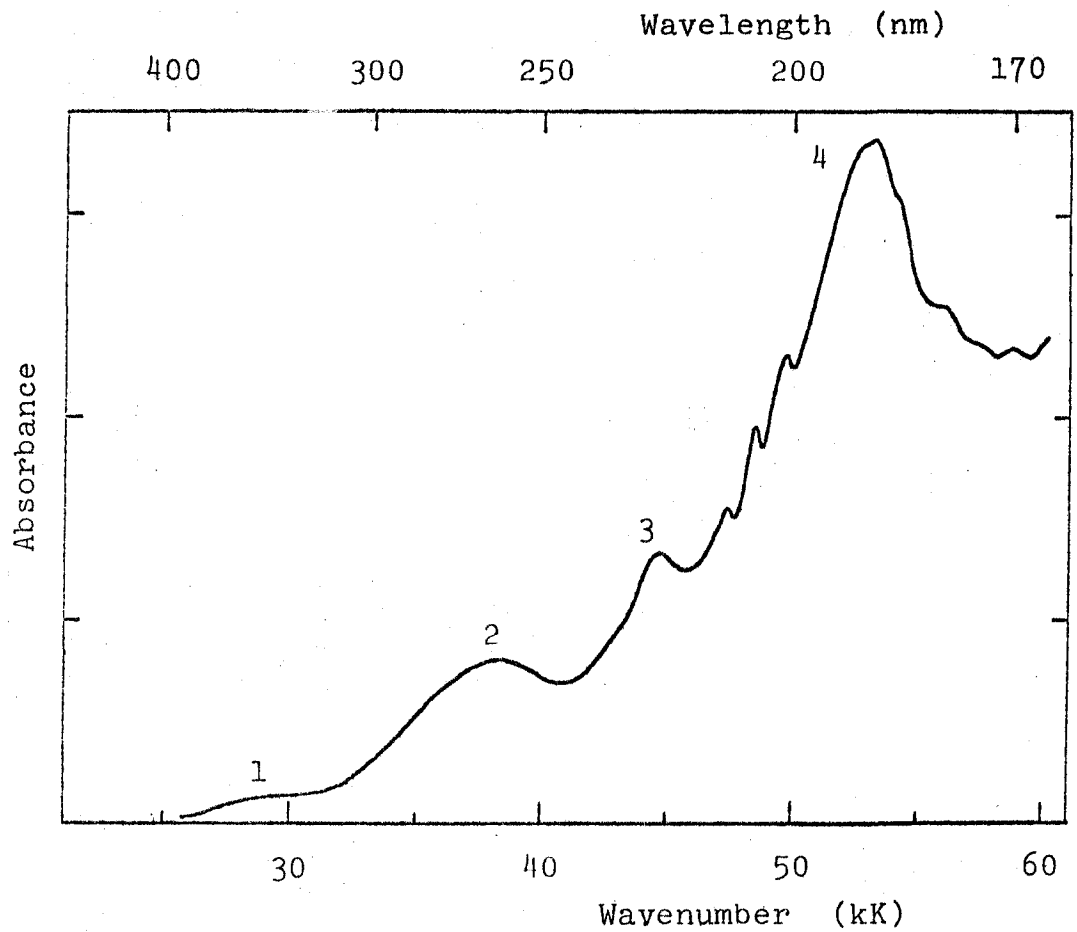

Fig. 1. The absorption spectrum of TMAE in the vapor.

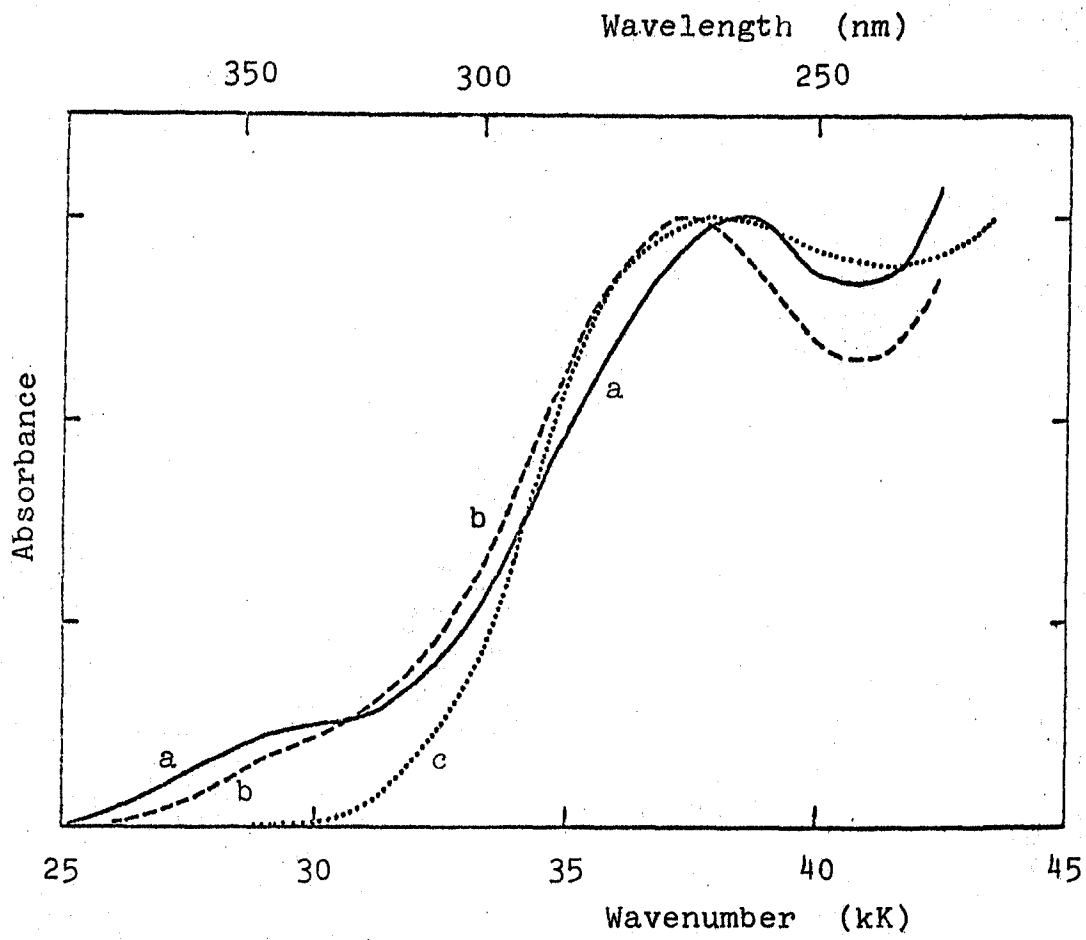

Fig. 2. The absorption spectra of TMAE in the near UV region; curve a (——) for the vapor, curve b (----) for an MP solution at room temperature and curve c (·····) for the same solution at 77°K. The profile around the second band (38 kK) of curve c is somewhat ambiguous, because the matrix became a little opaque.

The absorption maxima previously reported are 37.3 kK in n-heptane, tetrahydrofuran and acetonitrile,[5] and 37.0 and 45.2 kK in n-decane.[8] The agreements are good.

Absorption spectra of TMBI both in the vapor and in a n-pentane solution are shown in Fig. 3. Vapor absorption begins at about 25.0 kK and increases toward higher wavenumbers with a few inflexions (32.8 not clear, 35.7, 40.8 kK). The first peak is located at 50.5 kK. The second seems to exist at around 60 kK or higher.

It should be noted here that the first band of TMAE shifts to higher wave numbers in an MP solution at room temperature compared with that in the vapor although the second band shifts rather inversely and that the first band is apparently missing at 77°K. The absorption spectrum at wavenumbers lower than 45 kK for TMBI in the vapor is also apparently missing in a n-pentane solution.

Very recently, several studies concerning the Rydberg states in condensed media were made.[9,10] The main conclusion is that the Rydberg band is sensitive to the environments surrounding the molecule. It moves to shorter wavelengths when it is placed in the condensed phase or even in the gaseous state at high pressure.[11] The first band of TMAE and the bands in the near UV of TMBI show behaviors similar to the Rydberg bands reported in these studies, so that it may be concluded that they are Rydberg bands. It may

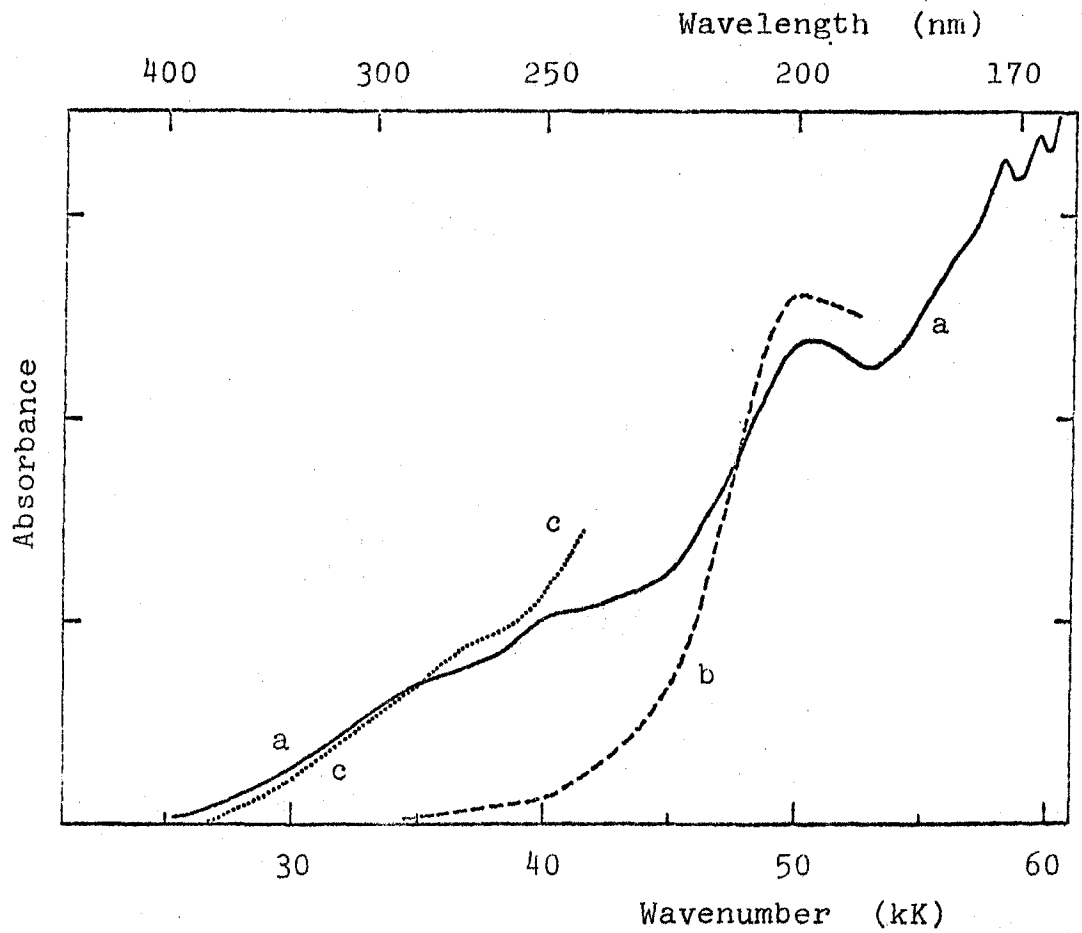

Fig. 3. The absorption spectra of TMBI; curve a (——) for the vapor, curve b (----) for a n-pentane solution at a low concentration of TMBI and curve c (·····) for the same one at a high concentration.

also be concluded that the second and third bands of TMAE and the 50.5 kK band of TMBI are non-Rydberg bands from their insensitiveness to the environments. The fourth band of TMAE also seems to be non-Rydberg, because it is too strong to be assigned to the Rydberg band. This conclusion is supported by the molecular orbital calculation.

It must be pointed out here that the gas-phase absorption spectrum of TMAE seems to contain an underlying continuous absorption which increases in intensity towards higher wave numbers, as seen in Fig. 1. This may be concluded to correspond to the transitions to the higher Rydberg series and the ionization-continuum. A similar feature is seen for the gas-phase spectrum of TMBI in Fig. 3.

Figure 4 shows the photo-ionization curves for TMAE. Curve a shows the relative photo-ionization cross section, σ_i^{rel}, as a function of photon energy, E, and curve b is the first derivative curve ($d\sigma_i^{rel}/dE$ vs E). σ_i^{rel} was calculated at every 10 Å by using the equation, $\sigma_i = \sigma \cdot i/(I_0 - I)$, where σ, i and $I_0 - I$ are the relative absorption cross section, photocurrent and relative light intensity absorbed by the sample vapor, respectively. The onset of the ionization is rather gradual. Such a feature is common to those reported for aliphatic and aromatic amino compounds.[12,13] In such cases, it is difficult to determine the adiabatic ionization potentials accurately. The author has, therefore,

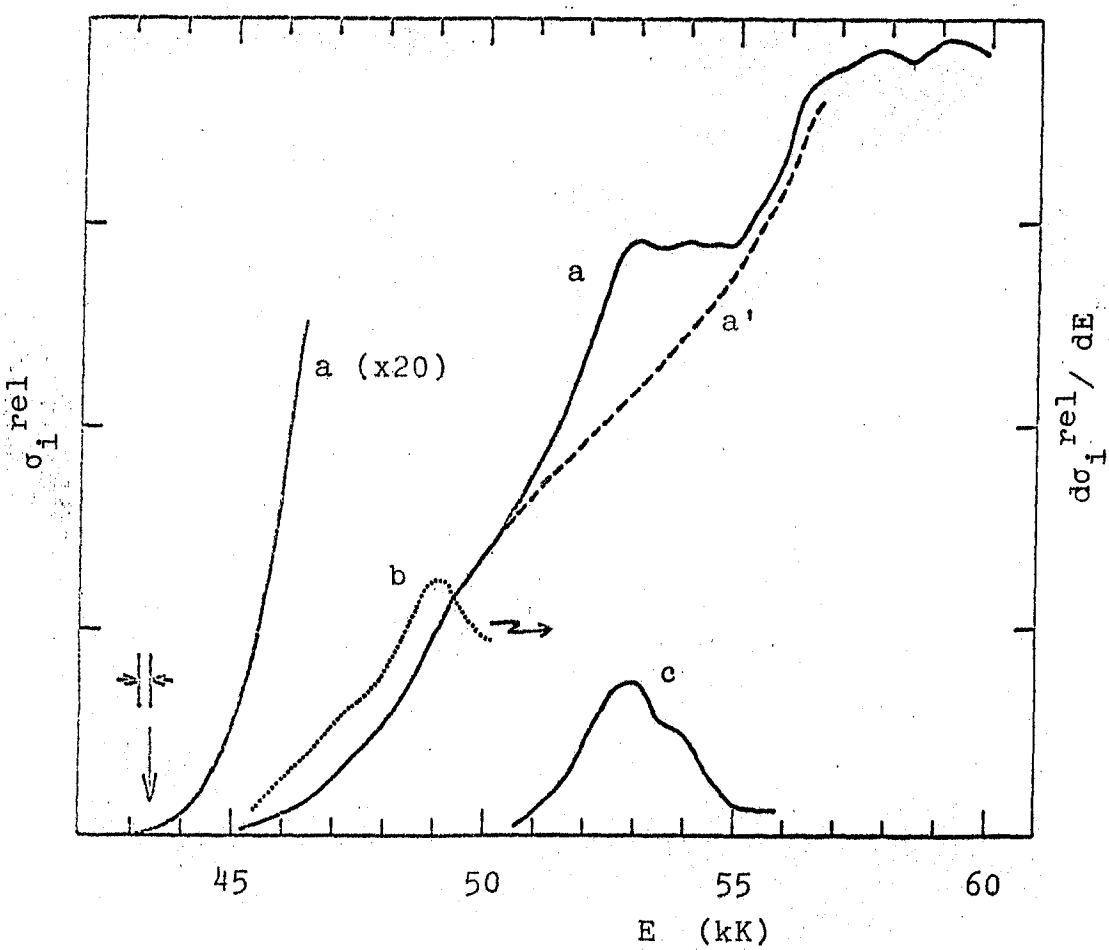

Fig. 4. Gas-phase photo-ionization of TMAE; curve a shows σ_i^{rel} vs E and curve b $d\sigma_i^{rel}/dE$ vs E. Curve a is divided into curve a' and c in the energy region around 53 kK, which are estimated to correspond to the contributions of the direct ionization and the auto-ionization, respectively. (See text.). The threshold for photo-ionization is shown by an arrow. The energy spread of the photon beam at the threshold is also indicated.

taken the point of appearence of σ_1^{rel} as an upper limit for the first adiabatic ionization potential.

Curve a has three steepest slopes at 49, 52 and 56 kK, and curve b has maxima at these positions, as shown only for the first steepest slope in Fig. 4. According to Morrison's method,[12] the first vertical ionization potential for TMAE can be determined to be 49.3 kK from the maximum of curve b. The second steepest slope at 52 kK, however, seems to be attributable to the auto-ionization from the fourth band of TMAE, rather than to the second (direct) ionization. The estimated curve for the direct ionization is shown as curve a' (a broken line) and the difference between the curves a and a' is shown as curve c, which corresponds to the contribution due to the auto-ionization. This interpretation may be supported by the fact that curve c agrees very well with the fourth band in Fig. 1. If this is the case, the second vertical ionization potential may be estimated to lie in 55 - 56 kK.

Photo-ionization curves for TMBI are shown in Fig. 5, from which the ionization potentials have been determined in the same way. The auto-ionization also seems to occur, but is not so clear. The first vertical ionization potential estimated to lie around 49 kK is, therefore, made somewhat uncertain. The second photo-ionization seems to start at about 57 kK.

Photo-ionization curves in the higher wavenumber

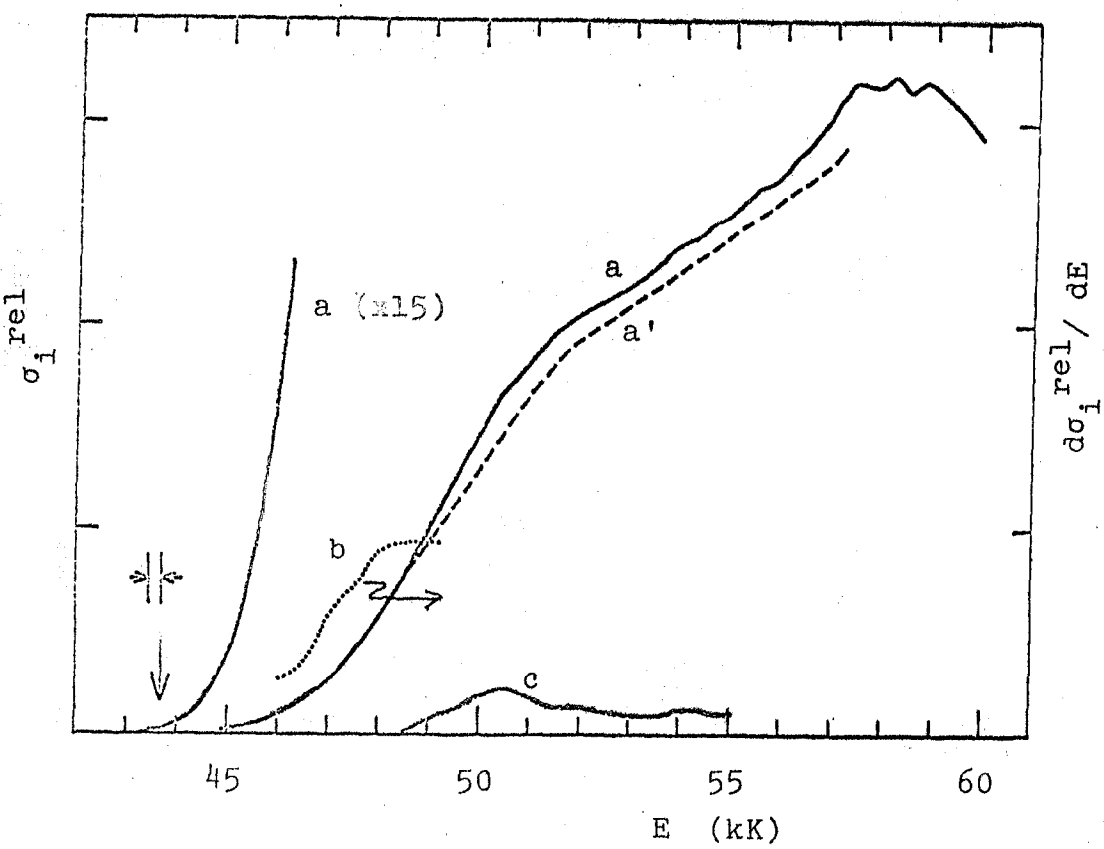

Fig. 5. Gas-phase photo-ionization of TMBI. Each curve and mark are indicated in the similar manner as in Fig. 4.

regions ($\gtrsim$57 - 58 kK), both in Fig's. 4 and 5, seem to be less reliable, because of the line spectrum of the hydrogen lamp used as the light source.

The ionization potentials are summarized in Table 1, together with those reported in the literature.

MO Calculations

In order to understand the experimental results, it seems worthwhile to make theoretical calculations of the electronic energies. For the purpose to find the orbital energies of filled π-MO's and to characterize the π-π* type transitions, a simple semi-empirical molecular orbital calculation was made using only the 2pπ-AO's on the C atoms and the lone-pair AO's on the N atoms. Each of the lone-pair AO's is assumed to be one of the sp^3 hybrid orbitals of the nitrogen atom. The details of the method of calculation is given in the Appendix.

The molecular conformations of tetraaminoethylenes have not been fully established. The planar $N_2C = CN_2$ skeleton can at least be assumed for the ground state. The inspection of the molecular model shows that the four dimethylamino groups have some freedom of twisting around each of the four C-N bonds. Let the direction of a C-N bond be the z-axis, and let us draw the projectories of carbon 2pπ-AO and nitrogen lone-pair AO on the xy plane as shown

Table 1. Gas-phase ionization potentials.

		the first Ip		the second Ip[c]
		adiabatic,	vertical	vertical
TMAE	this work	$\lesssim$5.36	6.11	ca. 6.9
	literature a)	$<$6.5		
	literature b)		6.27	
TMBI	this work	$\lesssim$5.41	~6.1	ca. 7.1

a), from the appearance potential of the parent ion in the mass spectrum; N. Wiberg and J. W. Buchler, unpublished.

b), calculated from the difference in the charge-transfer absorption maxima for TMAE and dimethylaniline as the donor(s) and nitrobenzene as the common acceptor, where 7.35 eV for the ionization potential of dimethylaniline was used; Ref. 15). This should be compared with the vertical value obtained by us.

c), These are only tentatively estimated values.

in Fig. 6 (A). Then, the angle θ as shown in Fig. 6 (A) can be the best parameter to define the conformation of the dimethylamino group. The C-N resonance interaction (β_{CN} in the Appendix) makes the "planar" structure ($\theta = 90^{\circ}$ in Fig. 6 (A)) the most preferable, which is, however, more or less prevented by the mutual steric repulsion between the crowded methyl groups. The infrared absorption spectrum of TMAE shows no band in the $\nu_{C=C}$ regions,[14] whereas an intense $\nu_{C=C}$ band (1630 cm^{-1}) appears in the Raman spectra.[7] TMAE also gives only one sharp proton signal in the NMR spectrum.[7,14] All these results suggest that the molecular conformation is symmetric with respect to the C=C bond. At present, the most reasonable model for TMAE in the ground state seems to be a "perpendicular" structure ($\theta = 0°$) under wobbly motion proposed by Hammond and Knipe,[15] in which the $(CH_3)_2N$ groups are vibrating about a position "perpendicular" to the $N_2C = CN_2$ plane. TMBI gives two sharp proton signals in the NMR spectrum. The steric repulsion between the methyl groups for TMBI seems to be much less than that for TMAE, but may still be large enough to prevent the complete "planar" structure.

The complexity of the problem arises from the fact that each of the four dimethylamino groups has a certain free domain of wobbly motion, and there are quite a number of possible conformations for TMAE. For TMBI, the situation

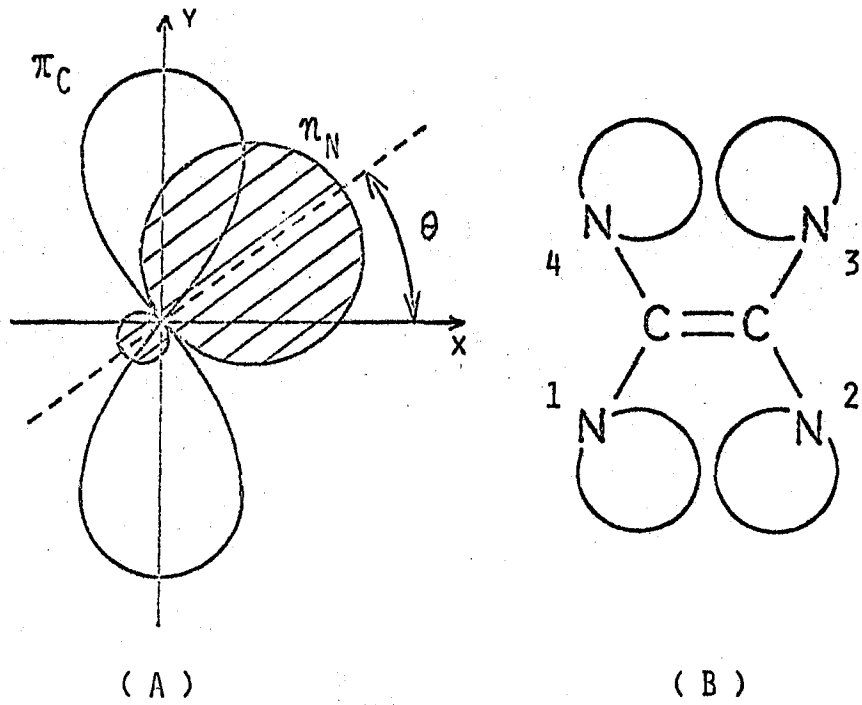

(A) (B)

Fig. 6. (A), A projection of a nitrogen lone-pair AO and a carbon 2pπ-AO on the xy plane perpendicular to the C-N bond. The angle θ is indicated. (B), The "perpendicular" structure of tetraaminoethylenes. Only the $N_2C = CN_2$ skeleton and four lone-pair orbitals are illustrated.

is somewhat similar, although there is a geometrical restriction of cyclization for the twisting motions. In order to describe various conformations, let us start from the "perpendicular" structure, in which all lone-pair orbitals lie on the $N_2C = CN_2$ plane in the manner as shown in Fig. 6 (B), and construct all other conformations by twisting dialkylamino groups about the C-N bonds with angles of θ_i, where i(=1,2,3,4) is numbering of dialkylamino groups as shown in Fig. 6(B). The angle θ_i is defined so as to have a positive value on twisting the lone-pair orbital upwards.

The calculation has been made for various possible conformations, i.e., at various θ_i values each independent of others. Part of the results obtained are shown in Fig. 7. Here, the molecular orbital energies are plotted as a function of θ for two types of conformations: (a), $\theta_1 = \theta_3 = -\theta_2 = -\theta_4$ (=θ) and (b), $\theta_1 = \theta_4 = -\theta_2 = -\theta_3$ (=θ). Each of these two types of conformations, especially (a), is expected to have the least steric repulsion between the methyl groups. The orbital energies of the four lone-pair orbitals are split by the direct N-N interaction into those of four MO's at the "perpendicular" structure ($\theta = 0°$). As the angle θ increases, this N-N interaction decreases, while the interaction between N and π_C becomes important. Consequently, somewhat complicated curves

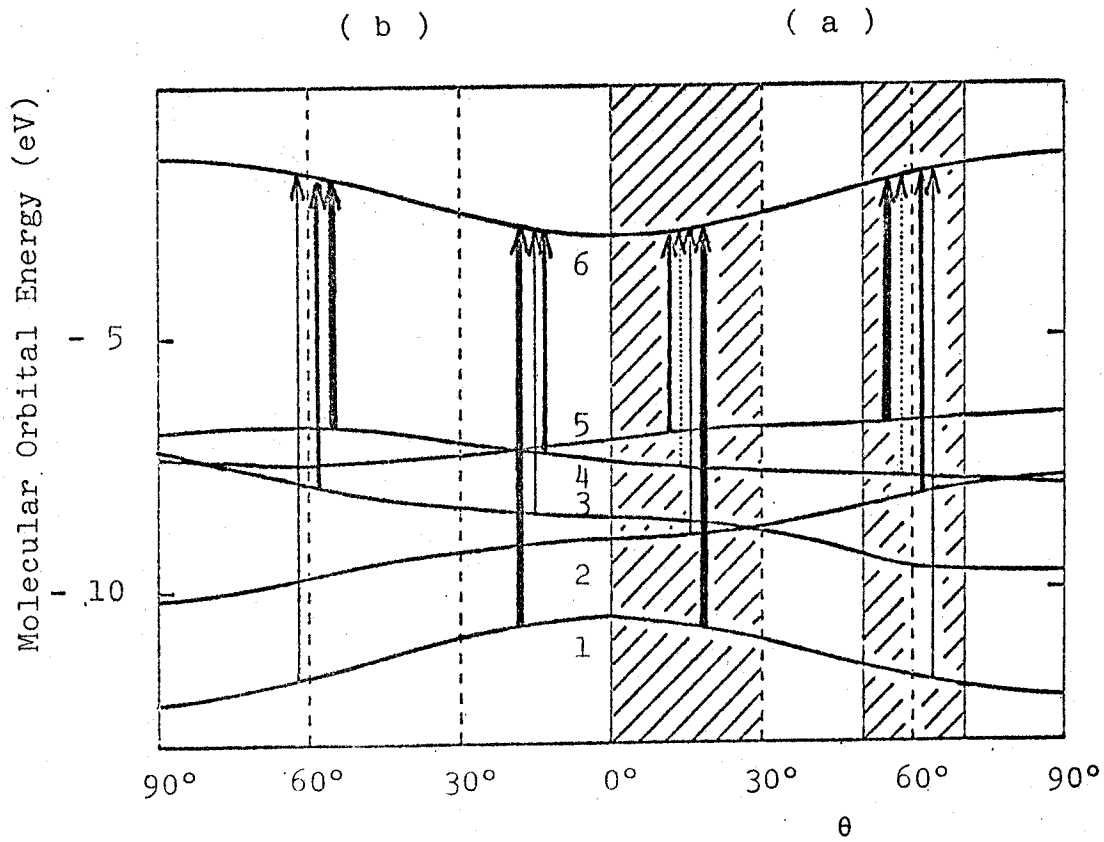

Fig. 7. Molecular orbital energies for tetraaminoethylenes. Each molecular orbital energy is plotted as a function of θ, for two types of conformations, (a) and (b). The Slater's parameter (μ) used is 1.80.

with several cross-points are obtained, as seen in Fig. 7.

Of the six MO's, which are numbered at $\theta = 0°$ as shown in Fig. 7, the lower five are filled with electrons, and only the highest is vacant. Allowed transitions under the approximation described in the Appendix[16] are indicated by arrows in Fig. 7; those having strong transition moments by thick arrows and those having weak transition moments by thin arrows. Arrows with dotted lines indicate those with negligibly small transition probabilities. The transition probabilities are found to depend strongly on θ. From the consideration of steric hindrances, it is assumed that the allowable region of θ for TMAE is from 0° to 30° and that for TMBI from 50° to 70°, which are marked by hatching for the conformation (a) in Fig. 7.

The results obtained are summarized as follows.

(1) The energy of the highest filled MO is nearly the same in the two regions; θ= 0° - 30° and 50° - 70°, as seen from Fig. 7. (Inversion of the highest filled MO's occurs for the conformation (b)). This result agrees with the observation that TMAE and TMBI have almost equal ionization potentials. The low ionization potentials of these molecules compared with the alkylamine and ethylene seem to be caused mainly by the direct N-N interaction for TMAE and mainly by the C-N resonance interaction for TMBI.[17]

(2) It is concluded in the previous section that the

first band of TMAE (Fig 1) is of Rydberg nature. From the results of calculation made for the conformation (a) in the region $0° \lesssim \theta \lesssim 30°$, it is shown that the $6 \leftarrow 1$ transition indicated in Fig. 7 is mainly of the nature of π-π^* transition in the ethylenic group and is therefore very strong. The transitions, $6 \leftarrow 5$ and $6 \leftarrow 2$, are shown to be forbidden at $\theta = 0°$ but become considerably strong near $\theta = 30°$.[16] The theoretical predictions for the relative intensities of these three transitions agree fairly well with those observed for the second, third and fourth bands in the TMAE absorption spectrum, though they are made somewhat ambiguous owing to the presence of the underlying continuum, as mentioned in the preceding section. The transition, $6 \leftarrow 4$, is predicted to be negligibly weak, and is probably hidden by other strong bands. Similar good agreements are also found for the conformation (b) in the region $0° \lesssim \theta \lesssim 30°$. (3) In the region $50° \lesssim \theta \lesssim 70°$, the transition energies are much larger than the corresponding transition energies at $\theta = 0° - 30°$ both for the conformations (a) and (b). This explains very nicely the marked blue-shift of absorption bands observed for TMBI compared with those for TMAE, since it has been concluded in the previous section that the 50.5 kK band of TMBI corresponds to the lowest allowed valence transition ($6 \leftarrow 5$ in Fig. 7(a) or $6 \leftarrow 4$ in Fig. 7(b)).

TMAE and TMBI have been assumed to take the structure

represented by either the conformation (a) or the conformation (b). These two conformations are expected to be preferred owing to their least steric repulsions between methyl groups. It might be possible, however, that TMAE and TMBI take structures represented by mixtures of these two and other conformations with the less steric repulsions between the methyl groups. Even in such cases, the above-mentioned conclusion is not substantially altered.

Discussion

The above mentioned calculated and observed results seem to provide fairly convincing explanation as to the question why TMAE and TMBI have nearly the same ionization potentials (Ip's), though they are expected to have different conformations.

Though the first vertical Ip's of TMAE and TMBI are easy to determine from the σ_i^{rel} curves, only the upper limits are obtained for the adiabatic Ip's. It seems, however, very likely from the following consideration that these observed limits lie close to the true adiabatic Ip's. The nuclear configuration of TMAE in the Rydberg state is expected to be similar to that of the positive ion, as pointed out for ethylene.[11] Therefore, the difference between the adiabatic and vertical energies for the Rydberg transition will be nearly equal to that for the

ionization. The difference between the vertical and adiabatic energies for the first Rydberg transition of TMAE is estimated fairly accurately to be about 0.6 eV, because the adiabatic energy for this transition can be obtained from the overlapping part of the absorption and fluorescence spectra. The difference between the observed limit for the adiabatic Ip and the vertical Ip determined in the present work for TMAE is about 0.7 eV as seen from Table 1, which is in fairly good agreement with the difference between vertical and adiabatic energies of the first Rydberg transition.

The large differences between the vertical and adiabatic Ip's for both TMAE and TMBI should be attributable to large change of the molecular conformations upon ionization. It is suggested that $TMAE^+$ has nearly "planar" structure from the ESR spectroscopic studies.[4, 18] It must also be pointed out that a large difference ($\sim$0.7 eV) was reported even for aliphatic amines,[13] possibly because of the change of the molecular shapes from the pyramidal structures to the planar.

The first band of TMAE and a number of low-lying bands of TMBI have assigned to the Rydberg bands on the basis of their characteristic behaviors in solutions compared with those in the vapor. The higher series for TMAE may be covered by the stonger second band corresponding

to the transition to the valence state. These unusually low-lying Rydberg states for tetraaminoethylenes are naturally expected from their very low Ip's.

The term values of Rydberg states in molecules fall into a series, expressed in the form,

$$T = R\,Z^2/(n^*)^2 = R\,Z^2/(n - \delta)^2,$$

where, Z is the charge on the core, R the Rydberg constant, n* the effective principal quantum number. From this equation, and using the adiabatic Ip and the wavelength at the center of the overlap between the first absorption band and the fluorescence spectrum, n* is calculated to be 2.3. If this band is assumed to be the first member of the series (n = 3), δ then becomes 0.7. The empirical δ-values reported for the Rydberg series of molecules built-up from atoms of the first period are 0.9 - 1.2 for ns-series, 0.3 - 0.5 for np-series and 0.1 for nd-series.[19] Deviation of the quantum defect, δ, for the first Rydberg state of TMAE from either those for ns or np-series, as seen above, may be attributable to the large departure of the core potential from spherical symmetry. The size of the Rydberg MO can be roughly estimated from the equation, $r_0 = (n - \delta)^2\, a_0/Z$, where a_0 is 0.529 Å and r_0 is the r-value at which the radial density has its maximum. r_0 = 2.9 Å is obtained for the first Rydberg state of TMAE. On the other hand, it is thought that the positive charge

of the core is located mainly on the four equivalent N atoms, since the highest filled MO consists mainly of the four lone-pair orbitals on the N atoms. The size of the core is, therefore, comparable with r_0 obtained above, since the N-N distances of TMAE are about 2.7 and 2.4 Å.

A large Stokes' shift between the first absorption and fluorescence bands is observed for TMAE. This large Stokes' shift was attributed by some authors to the conformational change of the fluorescent state of TMAE from the ground state, in the former of which the two N_2C halves are assumed to be perpendicular to each other in the $N_2C = CN_2$ skeleton.[4, 9] This explanation seems to assume that the first band is due to a π-π^* type transition. As discussed in the foregoing of this section, however, it seems more likely that the fluorescent state takes a structure similar to $TMAE^+$, in which the planarity of the skeleton is maintained.

Appendix.

A simple LCAO MO theory is used in this work. Normalized symmetry orbitals, ξ_i, are first constructed as follows,

$$\xi_1 = (2 + 2S_{CC})^{-1/2}(\chi_{Ca} + \chi_{Cb})$$
$$\xi_2 = (2 - 2S_{CC})^{-1/2}(\chi_{Ca} - \chi_{Cb})$$
$$\xi_3 = 2^{-1}(\chi_{N1} + \chi_{N2} + \chi_{N3} + \chi_{N4})$$
$$\xi_4 = 2^{-1}(\chi_{N1} + \chi_{N2} - \chi_{N3} - \chi_{N4})$$
$$\xi_5 = 2^{-1}(\chi_{N1} - \chi_{N2} - \chi_{N3} + \chi_{N4})$$
$$\xi_6 = 2^{-1}(\chi_{N1} - \chi_{N2} + \chi_{N3} - \chi_{N4})$$

where χ_{Ca} and χ_{Cb} indicate the two 2pπ-AO's on the C atoms of the C=C group and χ_{Ni} the lone-pair AO on the i-th N atom (Fig. 6(B)). The MO's of the whole molecule, ϕ, are, then, expressed as follows,

$$\phi = \Sigma\, c_i \xi_i$$

where c_i is a proper coefficient. The overlap integrals, S_{NN} and S_{CN}, are neglected, while S_{CC} is included and taken to be 0.257.

The two matrix elements, H_{11} and H_{22} ($H_{ii} = \int \xi_i H \xi_i d\tau$ where H indicates the effective one-electron Hamiltonian of the whole molecule), are assumed to be equal to - 10.5 and - 3.0 eV, respectively, empirically from the ionization potential and the excitation energy to the first excited singlet ($^1\Sigma_u^+$) state of ethylene. The four matrix elements, H_{33}, H_{44}, H_{55} and H_{66}, are given as simple sums of the nitrogen Coulomb integral, α_N, and various resonance

integrals between two nitrogen atoms, β_{NN}. α_N is taken to be - 8.0 eV from the vertical ionization potential estimated for $N(C_2H_5)_3$. The β_{NN}'s are found to play an important role in the case of TMAE and included in the calculation, although they were neglected in the MO calculations made for TMAE previously.[4] These integrals are calculated from the equations of the type, $\beta_{NN} = S_{NN}(\beta_{CC}/S_{CC})$, where S_{NN} is the overlap integral between two nitrogen atoms, and β_{CC} and S_{CC} are taken to be - 3.8 eV and 0.257, respectively. The calculation of S_{NN} is made by the use of Mulliken's table.[20] The Slater's parameter ($\mu = Z_{eff}/n^*$) for a nitrogen 2p AO calculated by ordinary Slater's rule is 1.95. However, a little smaller value may be more suited for a μ value of a nitrogen lone-pair AO. In the present work, calculations were made using two μ values of 1.95 and 1.80. It turned out that there was almost no substantial difference between the results obtained for the two μ values. The off-diagonal matrix elements, H_{ij} ($i \neq j$), are expressed in terms of β_{CN}, the resonance integral between the adjacent C and N atoms, which is calculated from the equation, $\beta_{CN} = 0.8\beta_{CC}\sin\theta$, where β_{CC} is taken to be - 2.5 eV by considering that the C-N distance is longer than the C=C distance of ethylene and θ is the twisting angle of the dialkylamino group defined before. The other parameters used are as follows; the bond distance, R(C=C) = 1.34 Å, R(=C-N) = 1.37 Å and the bond

angle, ∠NCN = ∠NCC = 120°.

Transition moments are calculated by assuming $\int \chi_p r \chi_q d\tau = 0$ if $p \neq q$. The center of the charge density of the lone-pair AO is assumed to lie at 0.3 Å away from the nitrogen neucleus in the direction of the sp^3 hybrid orbital.

References

1) K. Watanabe, T. Nakayama and J. Mottle, J. Quant. Spectry. Radiative Transfer, 2, 369 (1962); F. I. Vilesov, Usp. Fiz. Nauk. (SSSR), 81, 669 (1963). English Translation, Soviet Phys. USPEKHI, 6, 888 (1964).

2) Y. Nakato, M. Ozaki, A. Egawa and H. Tsubomura, Chem. Phys. Letters, 9, 615 (1971).

3) R. W. Hoffmann, Angew. Chem., 80, 823 (1968); Angew. Chem. Internat. Edit., 7, 754 (1968).

4) N. Wiberg, Angew. Chem., 80, 809 (1968); Angew. Chem. Internat. Edit., 7, 766 (1968).

5) M. Hori, K. Kimura and H. Tsubomura, Spectrochimica Acta, 24A, 1397 (1968).

6) For TMAE, R. L. Pruett, J. T. Barr, K. E. Rapp, C. T. Bahner, J. D. Gibson and R. H. Lafferty, Jr., J. Am. Chem. Soc., 72, 3646 (1950). For TMBI, H. E. Winberg, U. S. Patent, 3239518, 3239519 (1966).

7) H. E. Winberg, D. R. Downing and D. D. Coffman, J. Am. Chem. Soc., 87, 2054 (1965).

8) C. A. Heller and A. N. Flechter, J. Phys. Chem., 69, 3313 (1965).

9) B. Katz and J. Jortner, Chem. Phys. Letters, 2, 437 (1968), and the papers cited there.

10) A. J. Merer and R. S. Mulliken, Chem. Rev., 69, 639 (1969).

11) M. B. Robin and N. A. Kuebler, J. Mol. Spectry., 33, 274 (1970).

12) H. Hurzeler, M. G. Inghram and J. D. Morrison, J. Chem. Phys., 28, 76 (1958).

13) M. Batley and L. E. Lyons, Mol. Crystals, 3, 357 (1968).

14) N. Wiberg and J. W. Buchler, Z. Naturforsch., 19b, 5 (1964).

15) P. R. Hammond and R. H. Knipe, J. Am. Chem. Soc., 89, 6063 (1967).

16) The transition moments calculated for the conformation (a) under the approximation described in the Appendix are as follows, $\mu(6 \leftarrow 5)^2 : \mu(6 \leftarrow 4)^2 : \mu(6 \leftarrow 2)^2 : \mu(6 \leftarrow 1)^2 = 0.00 : 0.00 : 0.00 : 1.00$ at $\theta = 0°$; $0.69 : 0.00 : 0.29 : 0.54$ at $\theta = 30°$; $1.29 : 0.02 : 0.54 : 0.17$ at $\theta = 60°$; $1.45 : 0.04 : 0.56 : 0.08$ at $\theta = 90°$, where $\mu(n \leftarrow m)^2$ indicates the square of the transition moment from the m-th MO to the n-th MO in Fig. 7 relatively. The transition, $6 \leftarrow 3$, is symmetry forbidden for the conformation (a). The transition moments change continuously with θ. Similar results are obtained for the conformation (b).

17) Strictly speaking, the interaction with the σ-electrons must be included, especially at small θ. It is, however, expected from a simple consideration that this interaction causes little change for the highest filled MO in Fig. 7.

R. Hoffmann, A. Imamura, and W. J. Hehre, J. Am. Chem. Soc., 90, 1499 (1968).

18) K. Kuwata and D. H. Geske, J. Am. Chem. Soc., 86, 2101 (1964).

19) G. Herzberg, "Molecular Spectra and Molecular Structure III. Electronic Spectra and Electronic Structure of Polyatomic Molecules", D. Van Nostrand Co., Inc., Princeton, N. J., p. 341 (1966).

20) R. S. Mulliken, C. A. Rieke, D. Orloff and H. Orloff, J. Chem. Phys., 17, 1248 (1949).

Chapter II

Photo-Ionization and Rydberg States of Tetraamino-ethylenes in Organic Solutions

Summary

Absorption and emission spectra and photo-ionization curves of tetrakis-(dimethylamino)-ethylene, (TMAE), in some organic solvents have been measured. It has been found that the ionization thresholds for TMAE in n-pentane and benzene at 25°C lie around 4.20 ± 0.15 and $\lesssim$4.10 ± 0.15 eV, respectively, from which the energies of the excess electrons in these solvents are estimated to be slightly less than that of the free electron in vacuum (about - 0.2 eV in n-pentane). For TMAE in ether, an additional weak photo-current has been observed in the lower energy region, probably attributable to spontaneous formation of solvated electrons from the Rydberg states of TMAE in ether. Recombination processes from the Rydberg states and the ionization continuum to the fluorescent

state have also been concluded to occur from the fluorescence excitation spectrum. The Rydberg nature of the fluorescent state of TMAE, a conclusion which is consistent with the behavior of the first absorption band, has been deduced from the characteristic behaviors of the fluorescence spectra against the solvent rigidity and polarity. The fluorescence spectrum of TMAE in benzene has been tentatively assigned to a transition from a charge transfer state, where benzene molecules around TMAE act as electron acceptors.

Introduction

The photo-electron ejection from tetramethyl-p-phenylenediamine (TMPD) in rigid or fluid hydrocarbons occurs sometimes by the two-step, biphotonic processes with the lowest triplet state as the intermediate.[1-4] Cadogan and Albrecht determined the ionization threshold for TMPD in 3-methylpentane at 77°K, by monitoring the cation production spectroscopically, to be 5.9 eV,[5] only a little lower than the gas-phase, adiabatic ionization potential ($\lesssim$6.20 eV).[6, 7] They also reported that a weak, isotropic absorption from the triplet state extended from 380 to 470 nm, and interpreted it as due to the

transitions from the triplet state to the pseudo-Rydberg states.[8] Very recently, the ionization thresholds of TMPD in fluid n-hexane and tetramethylsilane were reported to be about 4.5 eV or higher from photo-current measurements by using monochromatic light.[3]

The photo-ionization phenomena of organic molecules in polar solvents are more complicated. Rather conflicting reports have been made by many investigators.[9-15] Recently, Ottolenghi summarized these data and proposed a mechanism in which two-step, biphotonic processes with the "semi-ionized" state as the intermediate take place.[15]

Recent observation of transient photo-currents induced by laser illumination in several fluid silanes and hydrocarbons showed the appearance of photo-ejected electrons with relatively high mobilities, 0.02 - 93 $cm^2V^{-1}sec^{-1}$.[3] Similar results have been observed by other techniques.[16] The formation of mobile (or "dry") electrons as precursors of trapped or solvated electrons both in polar rigid matrices at 77°K and in water at room temperature has also been proposed as a result of the radiolysis of these fluids or matrices.[17]

The study of the Rydberg states in relation with the ionization continua in amorphous media seems to be of growing importance, but still undeveloped at present.[18] Recently, it was reported that the lowest Rydberg states

of ethylene, acethylene and benzene were observed in rare gas matrices at 20° or 40 °K.[19, 20] The absorption bands corresponding to the transitions to these states showed appreciable blue-shifts relative to those in the gas phase, and the results were interpreted in a similar way as those for the atomic impurities in rare gas solids.[21] A new band appearing at 1612 Å in a benzene-krypton system at 40 °K was also tentatively assigned to the transition to an n=3 Wannier state of the benzene impurity, from which the ionization threshold was estimated to lie at about 7.75 eV,[19] about 2.0 eV lower than the gas phase ionization potential. Similar blue-shifts (or apparent disappearances) were observed for the absorption bands of alkyl-substituted ethylenes[22] and other small organic compounds[23] in the form of thin films or organic glasses, and for some bands of organic molecules in inert gases at high pressures,[22,24] and were attributed to the Rydberg nature of these bands. It was also reported that the large red-shifts in the fluorescence spectra of alkylamines in polar solvents could be explained as due to solvation for the Rydberg fluorescent states.[25]

The author found that tetrakis-(dimethylamino)-ethylene, (TMAE), has remarkably low gas-phase ionization potential of about 5.4 eV together with very low-lying Rydberg states.[7,26] In this chapter he is going to present

and discuss the results of measurements of absorption and emission spectra and photo-ionization curves of TMAE in organic solutions.

Experimental

The preparation and handling of TMAE, which is highly reactive with atmospheric oxygen, were described previously.[26] n-Pentane, isopentane and methylcyclohexane were also purified in the same way as described previously.[26] Ether was purified by shaking with a 10 % sodium bisulfite solution for two hours, then washed successively with 0.5 % sodium hydroxide, dilute sulfuric acid and saturated sodium chloride solutions, dried with calcium chloride, refluxed with sodium wire and distilled through a Widmer column. Tetrahydrofuran was left overnight in contact with sodium wire, refluxed for several hours with new wire and distilled through a Widmer column. Commercially available benzene was purified by shaking successively with concentrated sulfuric acid until free from coloring, then washed with water, dilute sodium hydroxide and water, followed by drying with calcium chloride. The benzene was crystallized three times in ice-water bath; one-fourth was discarded each time as unfrozen liquid. It was then dried with sodium wire and distilled through a Widmer column. These solvents were further dried with sodium

mirrors in ampoules connected to a vacuum line just before use. The air contained in solvents was removed before TMAE was dissolved.

Absorption spectra were measured with a Cary Model 15 spectrophotometer. Emission spectra were measured with an Aminco-Bowman spectrophotofluorimeter. Steady state photo-currents were measured as functions of photon energy. A 500 W Xenon dc lamp and a Shimadzu grating monochromator (F 3.5) were used for the photo-ionization. The half-width of the monochromatized light was normally 10 or 5 nm. Toshiba glass filters were used in front of sample cells when required to remove higher order or scattered light. The spectral distribution of the light intensity at the cell position was determined by use of a photomultiplier coated with sodium salicylate thin film. A quartz sample cell with two platinum-plate electrodes (10 X 40 mm) held parallel to each other by tungsten wire-glass seals was used for the measurements of both photo-currents and absorption spectra, from which relative concentrations of TMAE were determined. The measurements of steady state currents were made with a commercial picoammeter.

Results

Absorption and fluorescence spectra of TMAE in various solvents and in the gas-phase are shown in Fig. 1.

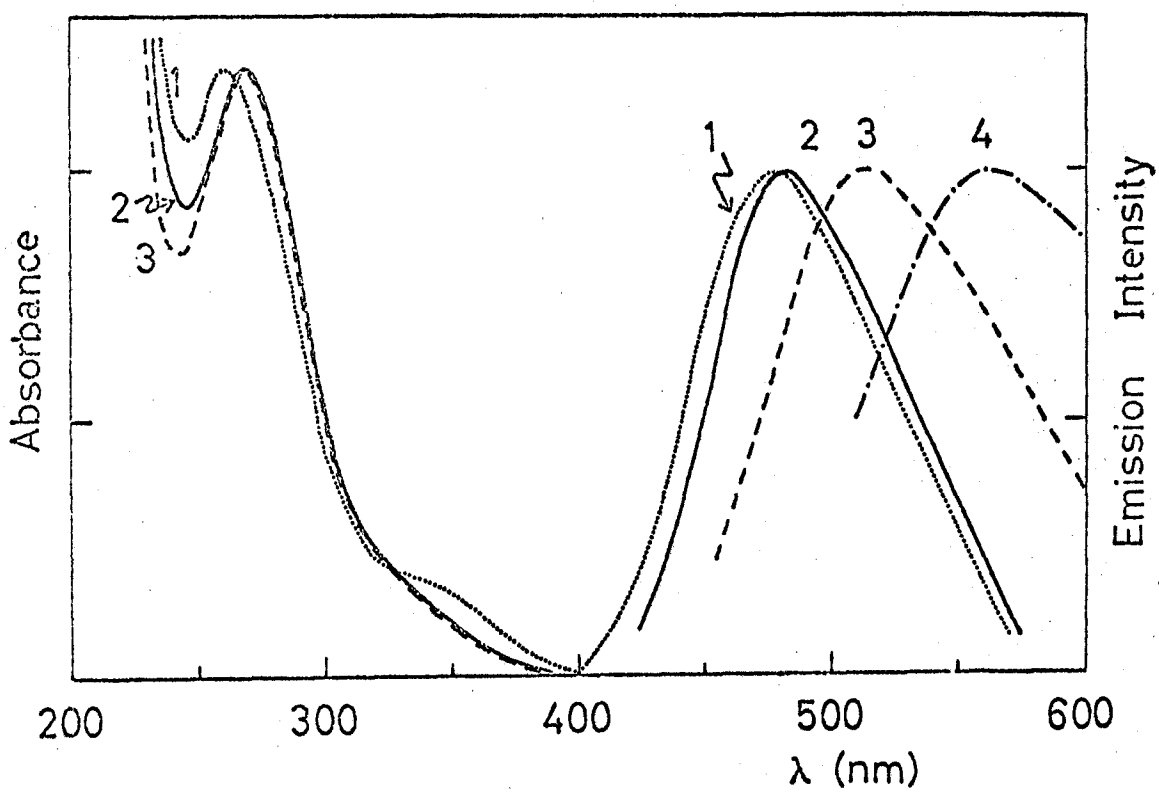

Fig. 1 Absorption and fluorescence spectra of TMAE; curve 1 for the vapor, curve 2 for the MP solution, curve 3 for the ether solution and curve 4 for the THF solution. Fluorescence intensities are normalized at the fluorescence peaks (see text), and are corrected for the spectral sensitivity curve of the photomultiplier used. Excitation wavelengths range from 390 to 250 nm, on which the positions and shapes of fluorescence spectra do not depend.

It should be noted that the absorption spectra in MP, ether and tetrahydrofuran (THF) are almost identical with each other though the spectrum in THF is not included in Fig. 1 to avoid complication. Here, MP is a mixed solvent consisting of methylcyclohexane and isopentane in a volume ratio of 1 : 1. The shoulder of the gas absorption spectrum at about 350 nm seems to be blue-shifted in the solution spectrum. The absorption spectra in the gas phase and in the MP solution have been already described and discussed in a previous chapter.

The fluorescene spectrum in the gas-phase shows a maximum at 477 nm and is rather strong. The fluorescence spectrum in the MP solution is also fairly intense and shows slight red-shift relative to that in the gas-phase. In polar solvents, however, the fluorescence spectra show large red-shift in the fluorescence maximum (λ_{max} = 486 nm (MP), 514 nm (ether) and 564 nm (THF)) and remarkable decrease in emission intensity (the relative fluorescence intensities in MP, ether and THF are roughly 1.00 : 0.2 - 0.1 : 0.05 - 0.01, respectively). These tendencies become stronger with growing solvent polarity. The fluorescence spectra of TMAE reported in papers on the chemiluminescent reaction of TMAE with oxygen[27,28] show relatively good agreements with the present data.

Temperature effects on the absorption and fluorescence

spectra of TMAE in the MP solution are shown in Fig. 2. The first absorption band shown as a shoulder at room temperature is apparently missing in the MP rigid glass at 77°K. The fluorescence spectrum at 77°K shows large blue-shift (λ_{max} at 77°K is 441 nm) relative to that at room temperature, the intensity being nearly the same.

Absorption and fluorescence spectra of TMAE in benzene at room temperature are shown in Fig. 3, together with those in MP. The absorption spectrum in benzene has a definite shoulder in the region of 290 to 350 nm, compared with that in MP. The fluorescence spectrum in benzene (λ_{max} = 424 nm) shows remarkable blue-shift relative to that in MP or in the gas phase. The fluorescene intensity in benzene is somewhat weaker than that in MP.

Photo-currents for TMAE measured with steady illumination both in n-pentane and in ether are shown as functions of photon energy in Fig. 4, where the photo-current scale is normalized by dividing photo-currents by the intensity of illumination at each wavelength. As the photo-current for TMAE in n-pentane increases with photon energy rather gradually, it is difficult to determine the photo-current threshold accurately. The photo-current threshold for TMAE as determined from the present result is 4.20 ± 0.15 eV in n-pentane at 25°C.[29)]

The photo-ionization curve for TMAE in ether at 25°C

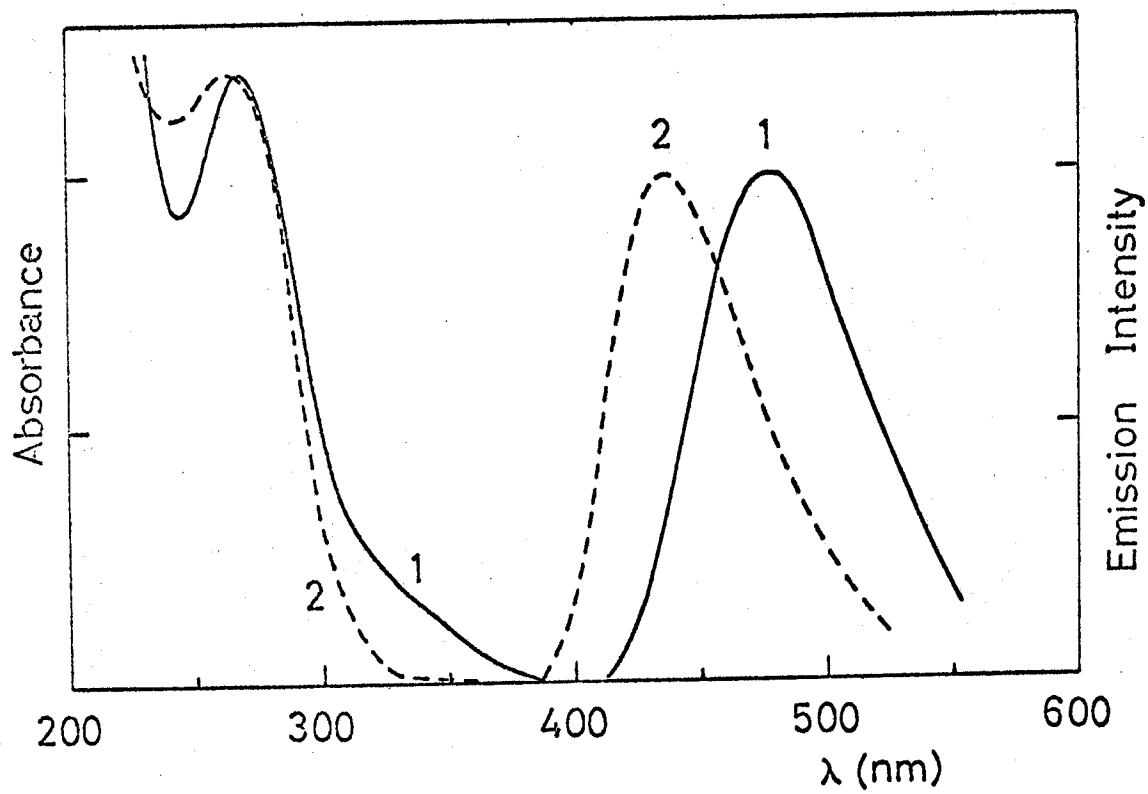

Fig. 2 Temperature effects on the absorption and fluorescence spectra of TMAE; curve 1 for the MP solution at room temperature and curve 2 for the same at 77°K. Spectra are illustrated in the same way as in Fig. 1.

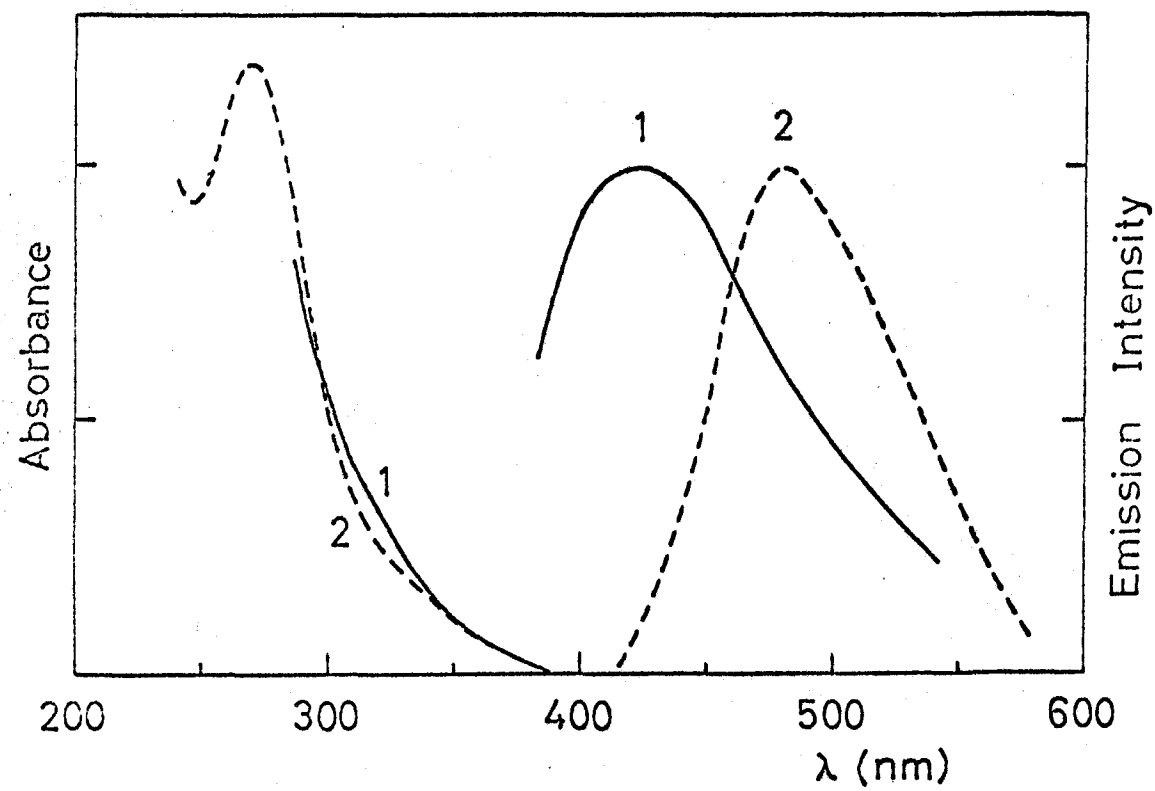

Fig. 3 Absorption and fluorescence spectra of TMAE; curve 1 for the benzene solution at room temperature, and curve 2 for the MP solution at room temperature. Spectra are illustrated in the same way as in Fig. 1.

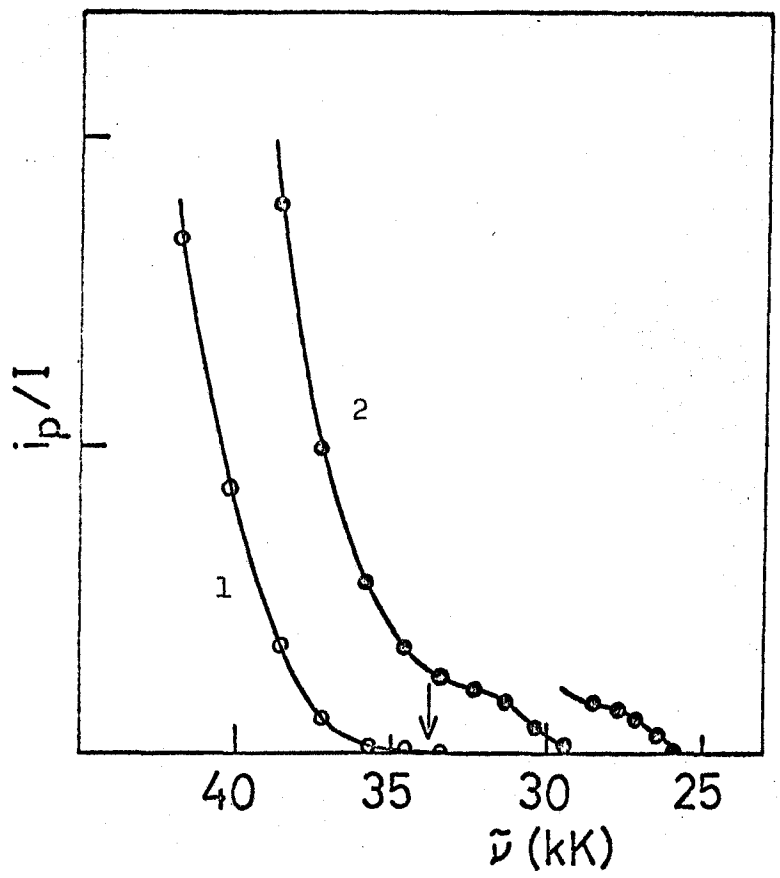

Fig. 4 Photo-ionization curves of TMAE in solutions; curve 1 for the n-pentane solution and curve 2 for the ether solution. I and i_p are the light intensity for excitation and the photo-current, respectively. The photo-current observed at the threshold, indicated by an arrow for the n-pentane solution, is about 2×10^{-13} A. Experimental points are denoted by circles. The half-width of light for the excitation is 10 nm. The electric field applied is ca. 400 V/cm.

shows considerable red-shift compared with that in n-pentane. It is to be noted that much larger photo-currents are observed in ether than in n-pentane, e.g., the ratio of the photo-current observed in ether to that in n-pentane at 270 nm is about 1000 in the same experimental condition.

It should be mentioned that the photo-current values shown in Fig. 4 involve the effect of the recombination processes of charge carriers.

The photo-current for TMAE in benzene has also been measured. The ionization threshold at 25°C is determined to be $\lesssim 4.10 \pm 0.15$ eV from the present work.[29] As the threshold lies very close to the onset of absorption of benzene, the photo-current can be measured in a very limited range of wavelengths.

Discussion

Ionization Thresholds in Non-Polar Solvents. ——— The potential energy for an electron ejected from a solute molecule into a non-polar solvent can be set as follows,

$$V(r) = - e^2/\varepsilon r + V_s \qquad (1)$$

where r is the distance between the electron and the center of the parent cation, ε the high-frequency dielectric constant of the solvent and V_s the potential energy of the electron due to the randomly oriented solvent. In the region where r is very large,

$$V(r) = V_s \qquad (2)$$

The ionization threshold for a solute molecule, M, in a solution, $I_s(M)$, might be defined as the excitation energy from the ground state of M to the bottom of the "ionization continuum".[30] Let us designate the energy of the electron lying at the bottom of the ionization continuum[30] with respect to that of a free electron at rest in vacuum as $E_s^o(e)$. $I_s(M)$ can be related with the gas phase ionization potential of M, $I_g(M)$, as follows (Fig. 5).

$$I_s(M) = I_g(M) + S(M) - S(M^+) + E_s^o(e), \qquad (3)$$

where S(M) is a solvation energy for M due to electronic polarization of the solvent and $S(M^+)$ that for the cation, M^+. There are "Rydberg" states or "Wannier-type exciton" states below the ionization continuum in the solution, which are the states of the cation-electron pair bound loosely by the Coulomb potential, $-e^2/\varepsilon r$. Only the lowest Rydberg state is indicated in Fig. 5.

The photo-current can be observed when a solute molecule is directly excited to the ionization continuum, whereas no photo-current should be observed when the solute is excited to the Rydberg states. The ionization threshold, $I_s(M)$, can, therefore, be determined experimentally from the threshold of the photo-current.[31]

Free charge carriers might be formed in some cases by

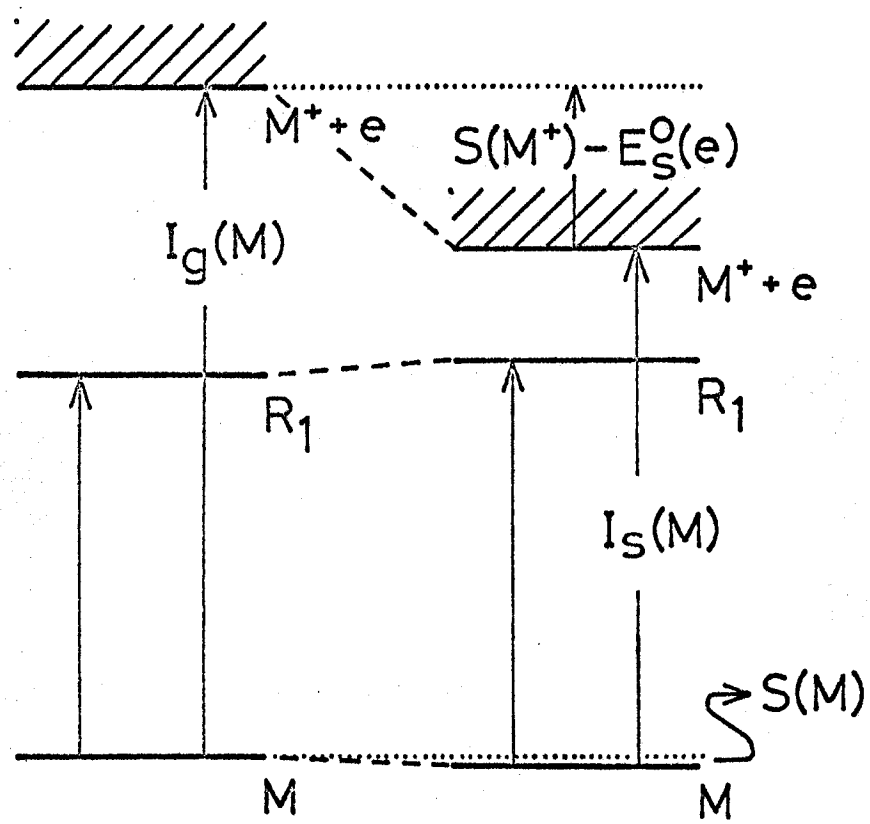

Fig. 5 The energy level diagram showing the ionization continua and the lowest Rydberg states of TMAE in the gas phase (left) and in the non-polar solution (right). Here, M, R_1 and M^+ are the ground state, the first Rydberg state and the cation of TMAE, respectively.

auto-ionization from discrete states lying above the ionization threshold to which the solute is first excited. For TMAE in n-pentane, the photo-current can be observed from ca. 295 nm, whereas the photo-ionization curve has no correlation with the absorption band observed at 270 nm in the same solution, as seen from Figs. 1 and 4. If the auto-ionization were to occur from the excited state corresponding to the 270 nm band, some swelling should be found in the photo-ionization curve at around 270 nm. Therefore, the photo-current for TMAE in n-pentane in this region seems to be due to the direct transition from the ground state of TMAE to the ionization continuum.

It is of great interest to note that $E_s^o(e)$, the ground state energy of the excess electron in n-pentane, can be estimated from our experimental values by using Equation (3). Taking 5.4 eV for I_g[7,26] and 4.2 eV for I_s, from the present results, and also estimating S(TMAE) to be 0.1 eV from heats of solutions of amino-compounds and $S(TMAE^+)$ to be 1.1 eV by applying the Born equation, where $TMAE^+$ is assumed to be a sphere of radius 3 Å, then $E_s^o(e) \approx -0.2$ eV is obtained. Similarly, the value of $E_s^o(e)$ in benzene can be estimated to be about - 0.1 eV by using 4.1 eV as I_s for TMAE in benzene. As discussed later, $E_s^o(e)$ in ether prior to dipole relaxation also seems to be nearly equal to that in n-pentane.

Although there are some reports on the electron mobility in organic media,[3,16] there have been no studies on another important quantity, the ground state energy of the excess electron in such media, $E_s^o(e)$. The present result is, to my knowledge, the first of the direct experimental derivation of such a quantity.[32] The values of $E_s^o(e)$ obtained might be qualitatively interpreted as follows. It is thought that the excess electron in n-pentane spends most part of its time in narrow vacant spaces between n-pentane molecules, based on the large, negative electron affinity of n-pentane. The electron will, therefore, have large kinetic energy in n-pentane, as an electron in a small box has, which is compensated by long-range polarization energy for the electron. Thus, $E_s^o(e)$ takes a small, negative value. Similar interpretation might be possible even for ether.

Benzene, unlike n-pentane, has lower vacant orbitals or, in other words, a small, negative electron affinity. It is also reported that benzene acts as an electron-trap in alkanes.[33] The physical nature of the excess electron in benzene may, therefore, be appropriately represented as a benzene anion whose site is moving from a benzene molecule to another. If this is true, $E_s^o(e)$ is approximated as $-EA(B) - S(B^-)$, where $EA(B)$ is the vertical electron-affinity of benzene and $S(B^-)$ the solvation energy for the

benzene anion due to the electronic polarization of benzene. Assuming EA(B) to be from - 1.0 to - 1.5 eV,[34] and estimating $S(B^-)$ to be 1.6 eV by use of the Born equation, $E_s^o(e)$ - 0.1 to - 0.6 eV is got, which agrees roughly with the observed value.

Ionization Thresholds in Polar Solvents. ——— When charged species are generated in polar solvents, orientational polarization follows immediately. The potential energy for the charged species, therefore, becomes a function of time, whose time constant is of the order of rotational motions of solvent molecules.[35] As the electronic excitation processes are much faster than such rotational motions, the excitation energies to the ionization threshold and the Rydberg states in polar solutions are regarded to be essentially the same as those in non-polar solutions.

The photo-ionization curve of TMAE in ether can be divided into two parts from inspection of Fig. 4; (a), a steeply rising part in the region higher than 35 kK, and (b), a shoulder in the lower energy region (35 - 25 kK). These two parts can be tentatively interpreted as follows: Part (a), due to the direct transition to the ionization continuum and Part (b) due to the spontaneous formation of solvated electrons from the Rydberg states of TMAE.

According to this interpretation, the photo-ejection

process in part (a) can be descibed as follows,

$$M \xrightarrow{h\nu} M^+ + e^- \qquad (4)$$
$$\searrow\!\!\sim\; M^+_{solv} \qquad \searrow\!\!\sim\; e^-_{solv}$$

Here, e^- means a mobile, not solvated, electron in the ionization continuum in ether. The photo-current threshold in part (a) should correspond to the bottom of the ionization continuum of TMAE in ether in the Franck-Condon state, lying at around 35 kK, nearly equal to that in n-pentane. It can, therefore, be deduced that $E_s^o(e)$ in ether is also nearly equal to that in n-pentane, because $S(M^+)$ in ether and in n-pentane should be nearly equal to each other before relaxation.

The process of spontaneous formation of solvated electrons from the Rydberg states can be described as follows,

$$M(R_{FC}) \rightsquigarrow M^+_{solv} + e^-_{solv} \qquad (5)$$

where $M(R_{FC})$ indicates molecule M in the Franck-Condon, Rydberg state. The process (5) includes trapping and solvation of the Rydberg electron whose orbital extends over solvent molecules, accompanied by their orientational motions. The energy required for the separation of the cation and electron is compensated by the solvation energies for them. Such a process is expected only in polar solutions and is interesting from the view-point of additional lowering of the ionization energies in polar

solvents, though the yield is not so large compared with that due to the direct transition to the ionization continuum.

It is to be noted here that the fluorescence excitation spectrum was found to extend up to higher energy regions, even beyond the ionization threshold for TMAE in ether (also in n-pentane and THF).[36] This suggests the presence of another process (6),

$$M(R_{FC}) \rightsquigarrow M^*_{fl} \qquad (6)$$

where M^*_{fl} indicates molecule M in the fluorescent state. Process (6) can be regarded as a sort of recombination luminescence. It is a process competing with process (5), causing weak fluorescence in polar solvents.

Solvent Effects on the Lowest Rydberg State. ——— The first absorption band of TMAE shown as a shoulder at 350 nm has been assigned previously[26] to the transition to the lowest Rydberg state, mainly from the blue-shift of the absorption bands in solutions relative to that in the gas phase. The fluorescence spectrum of TMAE described in this chapter can be concluded to originate from this lowest Rydberg state, based on the wavelength correlation between the first absorption band and fluorescence spectrum in the gas phase. It must be mentioned that such a lowest Rydberg state should be regarded as a state of "mixed valence shell-Rydberg character", strongly affected by

the core structure, as seen from the large quantum defect δ of 0.7 and from the relatively small size of the Rydberg orbital (r_{max} = 2.9 Å) described in the previous chapter.

The blue-shift (or apparent disappearance) of the first absorption band in solutions relative to that in the gas phase shows that the energy of the Franck-Condon, Rydberg state in solutions is higher than that in the gas phase, as shown in Fig. 5. This blue-shift might be caused by repulsive interactions between the electron in the Rydberg orbital and solvent molecules,[37] as mentioned qualitatively before. The more drastic change of the first absorption band in the MP rigid glass at 77°K compared with that in MP at room temperature is attributed to the increase of the density of the solvent MP at 77°K relative to that at room temperature.

The behaviors of fluorescence spectra in solutions can be explained as follows. In the non-polar solution at room temperature, it seems that the relaxation process of the solvent from the Franck-Condon state to the equilibrium fluorescent state leads to the expansion of the cavity within which the molecule in the Rydberg state is situated, so as to lower the repulsion between the solvent molecules and the electron in the Rydberg orbital. Thus, the fluorescence spectrum in the non-polar solution at room temperature appears in almost the same region of wavelength as that

in the gas phase. As such a relaxation process of the solvent is restricted in the rigid glass at 77°K, the fluorescence spectrum at 77°K is predicted to be at shorter wavelengths than the gas-phase spectrum, in agreement with the observation.

Another interesting feature is the large red-shift of fluorescence spectrum as the solvent becomes more polar. This is explained in terms of large stabilization due to the solvation of TMAE in the lowest Rydberg state, accompanied by the orientation of the solvents around the emitting molecule. A similar large red-shift has already been reported for the fluorescence of aliphatic amines in polar solvents, and explained in the same way.[25] It is to be noted that this "solvated Rydberg state" may be close to the "semi-ionized state" proposed as a photo-active intermediate in polar solvents by Ottolenghi.[11c,15]

Benzene Solutions of TMAE. ———— The result that the fluorescence spectrum of TMAE in benzene is apparently blue-shifted from that in the gas phase does not seem to be consistent with the reasonings made above. The absorption spectrum of this system shows a definite shoulder around 320 nm that is not found in the spectra for other solvents. These abnormalities for benzene are tentatively interpreted as being caused by a CT interaction between TMAE as a donor and benzene as an acceptor. The contact CT

absorption bands between TMAE and aromatic hydrocarbons such as pyrene, anthracene and perylene were observed at around 2.5 eV.[38] Since the difference of electron affinities between benzene and these aromatic hydrocarbons is estimated to be about 1.0 - 2.0 eV,[34,39] the contact CT absorption band between TMAE and benzene can be predicted to be at around 3.5 to 4.5 eV (or 350 to 280 nm), in good agreement with the position of the shoulder appearing in the absorption spectrum. The fluorescence spectrum seems to correspond well with this shoulder.

Based on the CT interaction above mentioned, schematic potential energy curves for TMAE in contact with a benzene molecule are shown in Fig. 6. The potential energy for the M···B pair arises from the normal van der Waals force and exchange repulsion force. For the R_1···B pair with the effective size of R_1 much larger than that of M, the repulsive exchange energy[37] sets in at distances larger than that for the M···B pair, as shown in Fig. 6. In the MP solution, the potential energy curve for TMAE in the Rydberg state in contact with the solvent molecule is thought to be similar to the R_1···B curve and it explains the blue-shift of the first absorption band compared with the gas-phase spectrum. On excitation, the relaxation process of the solvent schematically shown by an arrow with a dotted line in Fig. 6 takes place and, as the result, the fluorescence

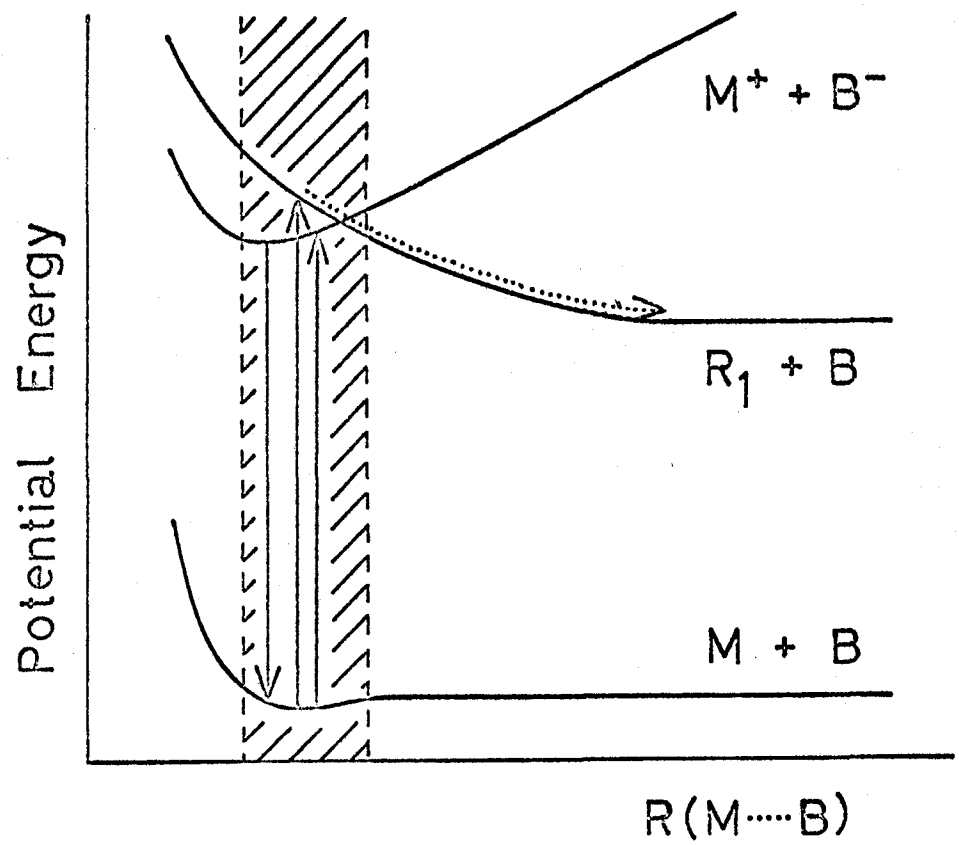

Fig. 6 Schematic potential energy curves for TMAE in benzene as a simple two-body problem. Here, M, R_1 and M^+ are the ground state, the first Rydberg state and the cation of TMAE, respectively. B is the ground state of benzene and B^- the benzene anion. R(M...B) means the distance between the TMAE and the nearest benzene molecule. The range of R(M...B) expected in the benzene solution of TMAE is indicated by hatching.

spectrum in MP does not shift appreciably from that in the gas phase. In the benzene solution, however, the CT configuration ($M^{+}\cdots B^{-}$) will play an important role at small distances, whose potential curve probably cross that for ($R_1\cdots B$). Thus, a potential minimum is expected to exist in the excited state. In the region of proper ($M\cdots B$) distances, indicated by hatching in Fig. 6, excited TMAE will fall into the potential minimum, from which the fluorescence is emitted. If the potential minimum is higher than the energy of separated states, (R_1 + B), the apparent blue-shift of the fluorescence is to be observed. Although the establishment of the above interpretation needs further work, this TMAE-benzene system seems to offer an interesting example for the study on the relation between the Rydberg state in the solution and the contact CT (or CT to solvent) state.

References

1) K. D. Cadogan and A. C. Albrecht, J. Chem. Phys., 51, 2710 (1969) and many papers cited there.

2) N. Yamamoto, Y. Nakato and H. Tsubomura, Bull. Chem. Soc. Japan, 39, 2603 (1966); 40, 451 (1967).

3) S. S. Takeda, N. E. Houser and R. C. Jarnagin, J. Chem. Phys., 54, 3195 (1971) and papers cited there.

4) M. Tamir and M. Ottolenghi, Chem. Phys. Letters, 6, 369 (1970).

5) K. D. Cadogan and A. C. Albrecht, J. Phys. Chem., 72, 929 (1968).

6) M. Batley and L. E. Lyons, Mol. Cryst., 3, 357 (1968).

7) Y. Nakato, M. Ozaki, A. Egawa and H. Tsubomura, Chem. Phys. Letters, 9, 615 (1971).

8) K. D. Cadogan and A. C. Albrecht, J. Phys. Chem., 73, 1868 (1969).

9) H. I. Joscheck and L. I. Grossweiner, J. Am. Chem. Soc., 88, 3261 (1966).

10) C. Hélène, R. Santus and P. Douzou, Photochem. and Photobiol., 5, 127 (1966); R. Santus, A. Hélène, C. Hélène and M. Potak, J. Phys. Chem., 74, 550 (1970).

11) For TMPD; a) Y. Nakato, N. Yamamoto and H. Tsubomura, Bull. Chem. Soc. Japan, 40, 2480 (1967); b) T. Imura, N. Yamamoto and H. Tsubomura, Bull. Chem. Soc. Japan,

43, 1670 (1970); c) R. Potashnik, M. Ottolenghi and R. Bensasson, J. Phys. Chem., 73, 1912 (1969); d) J. T. Richards and J. K. Thomas, Trans. Faraday Soc., 66, 621 (1970).

12) For pyrene and perylene; a) K. Kawai, N. Yamamoto and H. Tsubomura, Bull. Chem. Soc. Japan, 43, 2266 (1970); b) J. T. Richards, G. West and J. K. Thomas, J. Phys. Chem., 74, 4137 (1970); c) K. H. Grellmann, A. R. Watkins and A. Weller, J. Luminescence, 1,2, 678 (1970); d) R. Potashnik, Ph. D. Thesis, The Hebrew University of Jerusalem (1971); e) K. H. Grellmann, A. R. Watkins, Chem. Phys. Letters, 9, 439 (1971).

13) For naphtolate anion; a) M. Ottolenghi, J. Am. Chem. Soc., 85, 3557 (1963); b) C. R. Goldschmidt and G. Stein, Chem. Phys. Letters, 6, 299 (1970).

14) J. Joussot-Dubien and R. Lesclaux, Israel J. Chem., 8, 181 (1970).

15) M. Ottolenghi, a pre-print sent to the author

16) R. M. Minday, L. D. Schmidt and H. T. Davis, J. Chem. Phys., 54 3112 (1971) and papers cited there; Y. Maruyama, a private communication to the author .

17) a) From studies on electron and hole scavenging reactions; W. H. Hamill and his collaborators, J. Phys. Chem., 73, 1341, 2750 (1969); 74, 2885, 3914 (1970); Trans. Faraday Soc., 66, 2533 (1970); B. L. Bales, L. Kevan, J. Phys. Chem., 74, 1098 (1970); S. Arai, A. Kira and M. Imamura, ibid.,

74, 2102 (1970); b) From picosecond pulse radiolysis studies; M. J. Bronskill, R. K. Wolff and J. W. Hunt, J. Chem. Phys., 53, 4201, 4211 (1970); c) From studies on a recombination luminescence; H. B. Steen, J. Phys. Chem., 74, 4059 (1970).

18) Theoretical consideration on the Wannier exciton states in dense media; S. A. Rice and J. Jortner, J. Chem. Phys., 44, 4470 (1966).

19) B. Katz, M. Brith, A. Ron, B. Sharf and J. Jortner, Chem. Phys. Letters, 2, 189 (1968).

20) B. Katz and J. Jortner, Chem. Phys. Letters, 2, 439 (1968).

21) G. Baldini, Phys. Rev., 137, A508 (1965). See also, J.-Y. Roncin, N. Damany and J. Romand, J. Mol. Spectry., 22, 154 (1967).

22) A. J. Merer and R. S. Mulliken, Chem. Rev., 69, 639 (1969) and papers cited there; F. H. Watson, Jr. and S. P. McGlynn, Theoret. Chim. Acta (Berl.), 21, 309 (1971).

23) M. B. Robin, H. Basch, N. A. Kuebler, J. Chem. Phys., 51, 45 (1969); H. Basch, M. B. Robin and N. A. Kuebler, ibid., 51, 52 (1969); 49, 5007 (1968).

24) M. B. Robin and N. A. Kuebler, J. Mol. Spectry., 33, 274 (1970) and papers cited there.

25) Y. Muto, Y. Nakato and H. Tsubomura, Chem. Phys. Letters, 9, 597 (1971).

26) The first chapter.

27) A. N. Flecher and C. A. Heller, J. Phys. Chem., 71, 1507 (1967); N. Wiberg, Angew. Chem., 80, 809 (1968).

28) M. Hori, K. Kimura and H. Tsubomura, Spectrochimica Acta, 24A, 1397 (1968).

29) Strictly speaking, this should be regarded as an upper limit for the ionization threshold. Also see Ref. 31).

30) The electrons in the bottoms of the ionization continua in non-polar solvents such as n-pentane at room temperature seem to correspond to the relatively high mobility electron reported,[3,16] probably being in thermal equilibria with the solvents.

31) While the photo-ejected electron migrates away from the parent cation, it is frequently scattered by solvent molecules and loses part of its kinetic energy. This process decreases the yield of the current carriers. Therefore, precise determination of the true (or adiabatic) ionization threshold is rather difficult. L. Onsager, Phys. Rev., 54, 554 (1938); A. Mozumder and J. L. Magee, J. Chem. Phys., 47, 939 (1967); A. Mozumder, ibid., 48, 1659 (1968).

32) For rare gas liquids, the experimental and theoretical studies were reported; B. E. Springett, J. Jortner and M. H. Cohen, J. Chem. Phys., 48, 2720 (1968), and papers cited there.

33) K. Yoshinaga, N. Yamamoto and H. Tsubomura, J.

Luminescence, to be published; Also see for example, S. Khorana and W. H. Hamill, J. Phys. Chem., 74, 2885 (1970).

34) The electron affinity of benzene was reported to be about - 1.50 eV by theoretical calculations and by an electron scattering method. From the kinetics of electrode processes, - 0.54 and - 0.36 eV were also reported: J. B. Birks, "Photophysics of Aromatic Molecules", Wiley-Interscience, London (1970), p. 462.

35) The formation-time of a hydrated electron in aqueous solutions at room temperature was reported to be $\lesssim 10^{-11}$ sec from the pico-second pulse radiolysis studies.[17b)]

36) According to preliminary experimental results, no correspondence between the fluorescence excitation spectrum and the absorption band at 270 nm was observed both in the gas phase and in these solutions, showing absence of relaxation processes from the excited state at 270 nm to the fluorescent state.

37) The detailed nature seems to be very complicated. Deformation of the Rydberg orbital and also configurational mixings between the Rydberg state configuration and the charge-transfer-to-solvent configurations as well as the configurations in which the solvent molecule is excited must be taken into account. Here arises a question why the lowest Rydberg band is blue-shifted,

just opposite to the red-shift of the ionization continuum, as shown in Fig. 5. This seems to be explainable roughly by taking account of the decrease of the long-range polarization energy for the Rydberg states compared with the infinitely separated electron-cation pair (the ionized state).

38) P. R. Hammond and R. H. Knipe, J. Am. Chem. Soc., 89, 6063 (1967).

39) The adiabatic electron affinities of anthracene and pyrene were reported to be 0.42 or 0.552 eV and 0.39 or 0.579 eV, respectively, by an equilibrium electron capture method. R. S. Becker and E. Chen, J. Chem. Phys., 45, 2403 (1966). Also see Ref. 34). Strictly speaking, the vertical electron affinities should be used for CT absorption bands. Unfortunately, such data are unavailable at present.

Acknowledgments

I wish to express my sincerest thanks to Professor Hiroshi Tsubomura for his constant guidance and encouragement throughout the work. I am grateful to Assistant Professor Naoto Yamamoto for his helpful advice. My grateful thanks are also expressed to Professors and Doctors of this Department for their kind advice. I also wish to thank Mr. Masaru Ozaki for his active collaboration.

Publication List

1) "The Photo-ionization of N, N, N', N'-Tetramethyl-p-phenylenediamine in Organic Matrices", Hiroshi Tsubomura, Naoto Yamamoto, Katsumi Kimura, Toru Sato, Hikoichiro Yamada, Masahiko Kato, Gentaro Yamaguchi and Yoshihiro Nakato, Bull. Chem. Soc. Japan, 38, 2021 (1965).

2) "The Photo-ionization of Molecules in Solutions II Electron Transfer from Aromatic Diamine to Pyrene", Hiroshi Tsubomura, Naoto Yamamoto and Yoshihiro Nakato, Bull. Chem. Soc. Japan, 39, 1092 (1966).

3) "The Photo-ionization of Molecules in Solutions III Photo-ionization and Recombination Processes of N, N, N', N'-Tetramethyl-p-phenylenediamine in Various Organic Solvents", Naoto Yamamoto, Yoshihiro Nakato and Hiroshi Tsubomura, Bull. Chem. Soc. Japan, 39, 2603 (1966).

4) "The Photo-ionization of Molecules in Solutions IV Electron Capture and Charge Transfer Fluorescence Phenomena Occurring between N, N, N', N'-Tetramethyl-p-phenylenediamine and Electron Acceptors in Organic Solvents", Naoto Yamamoto, Yoshihiro Nakato and Hiroshi Tsubomura, Bull. Chem. Soc. Japan, 40, 451 (1967).

5) "The Photo-ionization of Molecules in Solutions V The Mechanism of the Photo-ionization of an Aromatic Diamine in the Polar Media", Yoshihiro Nakato, Naoto Yamamoto and Hiroshi Tsubomura, Bull. Chem. Soc. Japan, 40, 2480 (1967).

6) "Absorption Spectrum of Pyrene in the Excited Singlet State Measured by the Flash Method", Yoshihiro Nakato, Naoto Yamamoto and Hiroshi Tsubomura, Chem. Phys. Letters, 2, 57 (1968).

7) "Solvent Effects on the Fluorescence Spectra of Some Aliphatic Amines in Solutions", Yoshihiko Muto, Yoshihiro Nakato and Hiroshi Tsubomura, Chem. Phys. Letters, 9, 597 (1971).

8) "Organic Amino Compounds with Very Low Ionization Potentials", Yoshihiro Nakato, Masaru Ozaki and Hiroshi Tsubomura, Chem. Phys. Letters, 9, 615 (1971).